

PROMPT

UCPM-2022-PP/G.A-101101263

Work package 3 Del. Number D3.2

REPORT ON THE IMPLEMENTATION OF THE NUMERICAL MODELS

WP No	Del Rel. No	Del. No	Title	Description	Lead Beneficiar y	Nature	Dissemination level	Est.Del. Date
WP 3	D.3.2	D.7	Report on the implementation of the numerical models	Models implementation, model validation	UGE	Public Report	Public	31 October 2024

Summary

1. INTRODUCTION	6
1.1. Study Areas	7
1.2. General Methodology and Relation to Be-Ready	10
2. METOCEAN MODELLING	13
2.1. Hydrodynamic modelling.....	13
2.1.1. Model description	13
2.1.2. Model application	13
2.2. Atmospheric modelling.....	18
2.2.1. Model description	18
2.2.2. Model application	18
3. POLLUTION MODELLING: MARINE AND ATMOSPHERIC	21
3.1. Marine pollution modelling	21
3.1.1. Model description (TESEO)	22
3.1.1.1. Transport and Dispersion	22
3.1.1.2. Weathering processes for Oil spills	23
3.1.1.3. Weathering processes for HNS spills.....	23
3.1.2. Model implementation in each study case.....	24
3.2. Atmospheric pollution modelling	33
3.2.1. Model description	33
3.2.2. Model implementation	34
Generation of Meteorological Input Files	35
Simulation Runs and Postprocessing	35
3.2.2.1. Coupling between TESEO and HYSPLIT	35
4. RISK ASSESSMENT METHODOLOGY	37
4.1.1.1. Hazard.....	38
4.1.1.2. Vulnerability.....	39
4.1.1.3. Risk.....	42
4.1.1.4. Results.....	44



5. DECISION SUPPORT SYSTEM (DSS)	48
6. METHODOLOGY SUMMARY	55
7. REFERENCES.....	58



List of figures

Figure 1 - Plan view of the Genoa harbor's computational domain	8
Figure 2 - Plan view of the Tripoli harbor's computational domain	9
Figure 3 - Plan view of the Aqaba harbor's computational domain	9
Figure 4 - General framework of the system	11
Figure 5 - Features of the system implemented by site.	12
Figure 6 - On top: high resolution regular grid; down: bathymetry.	14
Figure 7 - Velocity field for scenario 01 at different time intervals, after 24, 72 and 120 hours from the initial time.	16
Figure 8 - Validation plots. On the left. Box plot of Normalized Root Mean Square Error, Hanna Heinold, Pearson Correlation, Skill coefficient; on the right: Taylor diagram.	17
Figure 9 - Typical output of the atmospheric modelling	19
Figure 10 - Atmospheric output structure	20
Figure 11 - Releasing positions for oil (top) and HNS (down) spills.	25
Figure 12 - Location of the spill points in the Port of Tripoli.	28
Figure 13 - Location of the spill points in the Port of Aqaba.	31
Figure 14 - Risk assessment model.	38
Figure 15 - ETA and hazard map for the HNS (on the left), and for the Oil (on the right).	45
Figure 16 - Physical vulnerability index for water pollution from OIL spills in the Port of Genoa.	46
Figure 17 - Environmental vulnerability index for water pollution from OIL/HNS spills in the Port of Genoa.	47
Figure 18 - Selecting the area of interest	48
Figure 19 - TESEO simulation form at PROMPT DSS	49
Figure 20 - Choosing the simulation scenario	50
Figure 21 - Results of the simulation	51
Figure 22 - Example of TESEO's trajectory results in Tripoli port area	52
Figure 23 - Pop-up window to launch atmospheric pollution simulation of the evaporated part of the substance	52
Figure 24 - Example of pollutant concentration between 0 and 10 m over the sea surface at Tripoli (left) and Aqaba (right) port area	53

List of tables

Table 1 - Oil spill points in Genoa.	26
Table 2 - HNS spill points in Genoa.	27
Table 3 - Oil spill scenarios selected in the Port of Tripoli.	29
Table 4 - HNS spill scenarios selected in the Port of Tripoli.	30
Table 5 - Oil spill scenarios selected in the Port of Aqaba.	32
Table 6 - HNS spill scenarios selected in the Port of Aqaba.	33
Table 7 - Physical vulnerability levels.	40
Table 8 - Environmental vulnerability levels.	40
Table 9 - Socio-economic vulnerability levels.	41
Table 10 - Human vulnerability levels.	41
Table 11 - Socio-economic vulnerability levels.	42
Table 12 - Hazard levels.	42
Table 13 - Risk weights.	43
Table 14 - Standardized risks.	43
Table 15 - Risk levels.	43
Table 16 - List of available substances for forecast on-demand in PROMPT DSS.	49
Table 17 - Models results and application.	56

1. INTRODUCTION

Pollution in the marine environment represents a significant threat to ecosystems, economies, and the well-being of coastal communities. In regions like the Mediterranean Sea, an area characterized by dense shipping traffic, industrial activities, and thriving tourism, the risks associated with accidental pollutant spills, such as oil or hazardous and noxious substances (HNS), are particularly acute. The complex interplay of environmental, economic, and social factors makes it essential to develop tools capable of predicting pollutant dispersion with accuracy and reliability. This predictive capability is critical for timely and effective response strategies that minimize environmental damage and socio-economic impacts.

This document presents the technical modeling framework developed as part of the PROMPT project, designed to simulate pollutant dispersion in key port areas of the Mediterranean Sea. The study focuses on three strategic locations, each chosen for its environmental and operational diversity:

- Port of Aqaba (Jordan): A vital gateway to the Red Sea, characterized by arid conditions and unique coastal dynamics.
- Port of Tripoli (Lebanon): A bustling hub for trade and commerce in the Eastern Mediterranean, facing seasonal variations in wind and current patterns.
- Port of Genoa (Italy): A major European port with complex hydrodynamic and atmospheric interactions, influenced by dense maritime traffic and proximity to urban areas.

The modeling framework is structured around two interconnected components:

1. **Metoccean Modeling:**

This component forms the foundation of the framework, simulating the physical processes that drive the movement of water and air in the marine environment. Hydrodynamic modeling captures the dynamics of ocean currents, tides, and waves, incorporating high-resolution bathymetry. Simultaneously, atmospheric modeling provides detailed simulations of wind fields, temperature, and other weather conditions that influence the transport and dispersion of pollutants. Together, these models offer a comprehensive representation of the environmental forces at play, ensuring that pollutant modeling is grounded in accurate, site-specific data.

2. Pollutant Modeling and Risk Assessment:

Building on the outputs of the metocean models, this component predicts the dispersion of pollutants, such as oil spills and HNS, in both the marine and atmospheric environments. The framework includes an advection-diffusion module for tracking pollutant transport and a weathering module that accounts for processes like evaporation, dissolution, emulsification, and sedimentation. To further enhance decision-making, a risk assessment methodology evaluates the hazard (extent and intensity of pollution), vulnerability (sensitivity of affected areas), and overall risk to marine and coastal ecosystems.

The goal of this document is to describe the methodologies, tools, and case studies underpinning this modeling framework. By simulating pollutant dispersion across diverse scenarios, the framework provides a solid foundation for improving our ability to anticipate the spread of pollution and its potential impacts. This knowledge is critical for supporting emergency planning, resource allocation, and effective response strategies in the event of spills.

A key innovation of the PROMPT project is the development of an **interactive web platform** that enables users to simulate pollutant dispersion scenarios tailored to specific incidents. Through this platform, users can define key parameters—such as pollutant type, release location, and quantity—and explore precomputed scenarios under realistic environmental conditions. By leveraging daily forecast data, the platform automatically identifies the most relevant hydrodynamic and atmospheric scenarios, ensuring that simulations are aligned with current conditions. This approach empowers decision-makers with actionable insights, enabling them to plan and respond to pollution incidents with precision and confidence.

1.1. Study Areas

The three study areas planned to focus on this project include the port of Genoa (Italy), the port of Tripoli (Lebanon), and the Gulf of Aqaba (Jordan).

The former sites are located in the Mediterranean Sea and the latest is in the Red Sea. The port of Genoa is located in the Ligurian Sea (Northwestern Mediterranean), latitude 44° 4' 03" N and longitude 8° 86' 2" E, is the largest commercial port in the Mediterranean Sea. The computational domain developed for this study covers the Gulf of Genoa, with the external boundary width equal to 80 km, and the distance from the port equal to 20 km (Figure 1).

The port of Tripoli geographically located in the Eastern Mediterranean Sea, Northern area of Tripoli city at $34^{\circ}27'03''\text{N}$ $35^{\circ}49'43''\text{E}$ is among the most important port on the eastern basin of the Mediterranean Sea since it serves as a link between East and West. Figure 2 shows computational domain used for port of Tripoli. The domain consists of a semicircle area with an arc length of 32 km radius of 9 km and, covering a distance of 5.6 km from the port's maximum protrusion to the open boundary.

The Gulf of Aqaba, located at $28^{\circ}45'\text{N}$ $34^{\circ}45'\text{E}$, is a narrow, deep and long most northern extension of the Red Sea. The gulf is the only access of Jordan to the sea and surrounded by dry desert mountains, no riverine inputs and only a negligible runoff. Computational domain utilized for modelling of Gulf of Aqaba is depicted in Figure 3. The domain covers a long and relatively narrow area with a length of 50 km and a variable width of 5 to 20 km from the northern part of the gulf to the offshore part, respectively.



Figure 1 - Plan view of the Genoa harbor's computational domain

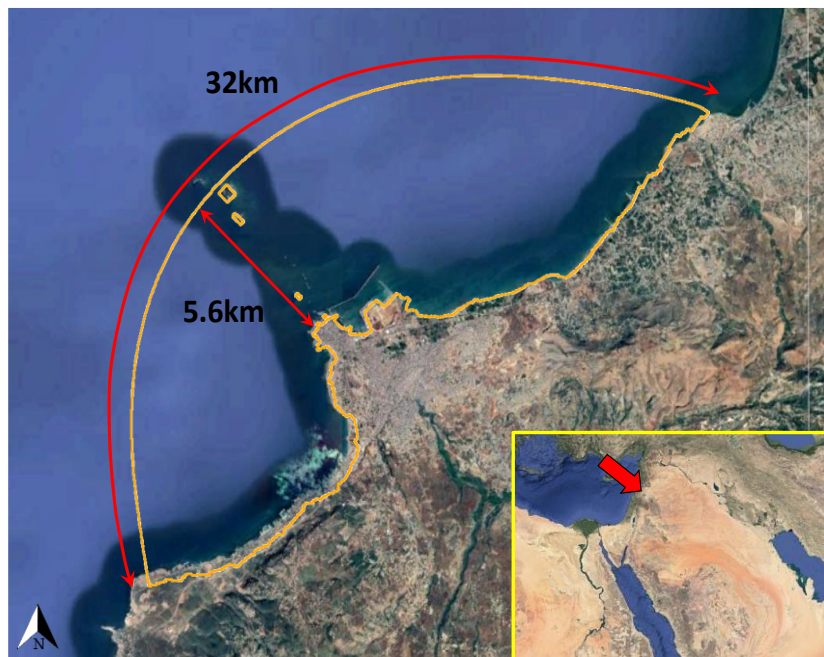


Figure 2 - Plan view of the Tripoli harbor's computational domain

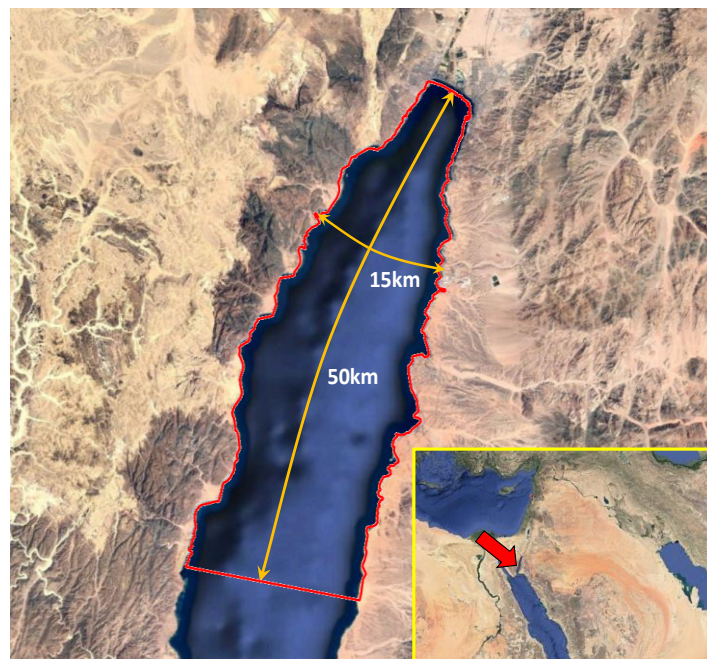


Figure 3 - Plan view of the Aqaba harbor's computational domain

1.2. General Methodology and Relation to Be-Ready

The Prompt system has been developed to be a valuable tool for facing marine pollution emergencies produced by oil and Hazardous and Noxious Substances (HNS) spills. To achieve this objective, the system comprises the following main elements (see Figure 4):

- i) High-resolution metocean data: to provide pollution modelling, it is necessary to know the main variables that dominate the processes of dispersion and evolution of the pollutants. For that reason, it is required to have a high-resolution modelling of the ocean currents and winds at the sites. These results are the first input of the pollutant modelling
- ii) Remote sensing for the identification of oil spills: thanks to remote sensing it is possible to monitor the sea to detect oil slicks even under varying weather conditions and during both day and night. Upon detecting an oil spill, remote sensing data allows operators to rapidly initiate on-demand simulations, utilizing the observed spill location as a starting point to forecast the pollutant's trajectory.
- iii) On-demand forecast modelling: the system provides the ability to model and predict the trajectory of oil and HNS spills and the evolution of the main physicochemical processes of the substance. Moreover, when a chemical substance produces evaporation, the system will analyze the evolution of the pollutant in the atmosphere using a coupling with an atmospheric pollution model. The core of the system is based on the spill numerical model TESEO developed by IHCantabria to simulate the fate, transport and dispersion of oil and chemical spills in the marine environment. TESEO is coupled to an air quality numerical model (HYSPLIT from NOAA) to predict the HNS evolution at the whole marine environment (seawater and atmosphere) (see more details in Section 3). As forcings, the system uses the pre-run metocean scenarios (described in step i) statistically representative of the variability of the study site. As result, the system provides in real time spill trajectories and weathering forecasting (with a maximum temporal horizon of 5 days) of oil and HNS spills in the marine environment as well as the forecasting of the dispersion in the atmosphere of the toxic cloud.
- iv) Oil and HNS Risk assessment system: the system provides hazard, vulnerability and risk maps, both in the marine environment and in the atmosphere, due to accidental oil and HNS spills. The risk is estimated as the combination of hazard

and vulnerability. Hazard is defined as the probability of the environment (marine and atmosphere) to be polluted by an oil/HNS spill. The hazard is calculated on the basis of a high number of numerical simulations that represent the metocean variability of the site (pre-run metocean scenarios mentioned in step i) and the potential spill scenarios. The numerical simulation of the evolution of the pollutant in the marine environment and in the atmosphere is carried out based on the aforementioned coupling between TESEO and HYSPLIT models. The vulnerability assessment integrates physical, biological, and socio-economical aspects as well as the vulnerability to the population. As a result, the system provides physical, environmental, socio-economic and risk maps to population, both for marine and atmospheric pollution. The risk assessment system provides valuable results for planning and preventing possible emergencies.

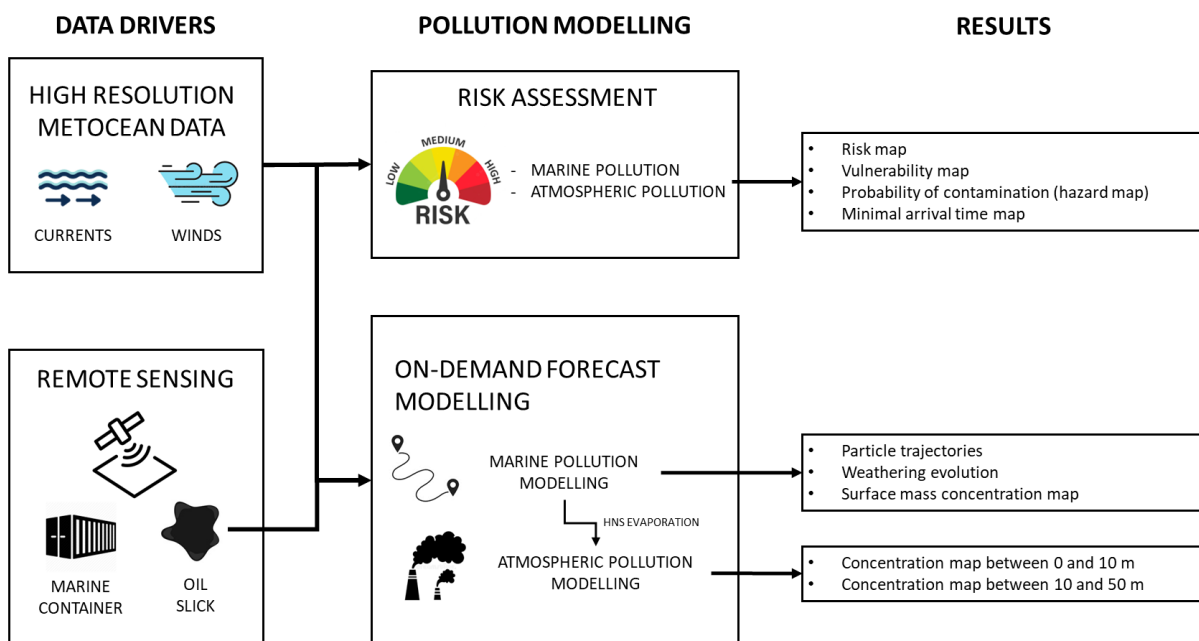


Figure 4 - General framework of the system

This project builds upon previous work carried out in the Be-Ready project while introducing new developments (marked in Figure 5 as “new”) in specific pilot sites. The main updates and distinctions are summarized as follows:

- **Genoa:** Fully new hydrodynamic modeling has been implemented. However, no atmospheric modeling has been included for this site.

- **Aqaba and Tripoli:** Hydrodynamic and atmospheric modeling were already implemented in Be-Ready. In this project, we have improved the wind input data by incorporating higher-resolution datasets.
- **La Spezia:** The hydrodynamic modeling from Be-Ready has been directly adopted without modifications or additional developments. No atmospheric modeling is included.

In addition to these site-specific updates, in Genoa, Aqaba and Tripoli, new **remote sensing techniques** have been applied to improve the identification of oil spills, and a new **risk assessment** methodology has been developed.

































	Genoa	Aqaba	Tripoli	Spezia
DSS INTEGRATION	  Genoa	 Aqaba	 Tripoli	 Spezia
HIGH-RES FORCINGS	 	 	 	
MODELLING ON DEMAND	 	 	 	
RISK ASSESSMENT (STATISTICAL)	 	 	 	
NEW REMOTE SENSING	 	 	 	

Figure 5 - Features of the system implemented by site.

2. METOCEAN MODELLING

2.1. Hydrodynamic modelling

Hydrodynamic models are essential tools for simulating water movement and understanding the physical processes governing coastal and marine environments. They allow us to analyze complex flow patterns driven by tides, wind, and other environmental forcings, providing valuable insights for pollutant dispersion studies.

In this project, we build on previous work carried out within the Be-Ready project, where the hydrodynamics of the pilot sites in Aqaba and Tripoli were already modeled and analyzed. Here, we focus on the Gulf of Genoa, the newly implemented site, describing the setup and results of its hydrodynamic simulation using the Delft3D 4 model, a widely used and well-established tool for coastal and estuarine studies.

2.1.1. Model description

For the Gulf of Genoa, the Delft3D-FLOW module was used to simulate water movement, considering the key forcings such as tides and wind. The model was implemented with a regular grid adapted to the coastline and bathymetry to ensure accurate representation of local hydrodynamics. A new clustering method was applied to collect and integrate environmental variables, improving the resolution of key physical processes.

The simulation setup included 11 sigma layers to represent vertical stratification, a time step of 0.05 minutes to ensure numerical stability, and a Chezy coefficient of $65 \text{ m}^{1/2}/\text{s}$ to parameterize bed roughness. The wind drag coefficient was set to 0.0063, and turbulence was modeled using the k- ϵ approach.

By refining the computational approach and integrating improved environmental data, this hydrodynamic model provides a solid basis for understanding pollutant dispersion in the Gulf of Genoa. The results will serve as a key input for the subsequent oil spill and particle dispersion simulations.

2.1.2. Model application

Grid and Bathymetry

A high-resolution grid was developed to match the coastal and underwater features of the Gulf of Genoa. The mesh consists of over 61000 cells, with a resolution ranging from 50 meters inside the port to 250 meters offshore.

Detailed bathymetric information downloaded from GEBCO provided accurate seabed data, interpolated using different methods depending on data density. The resulting depth map captures key underwater features, including two submarine canyons that influence local circulation (see Figure 6).

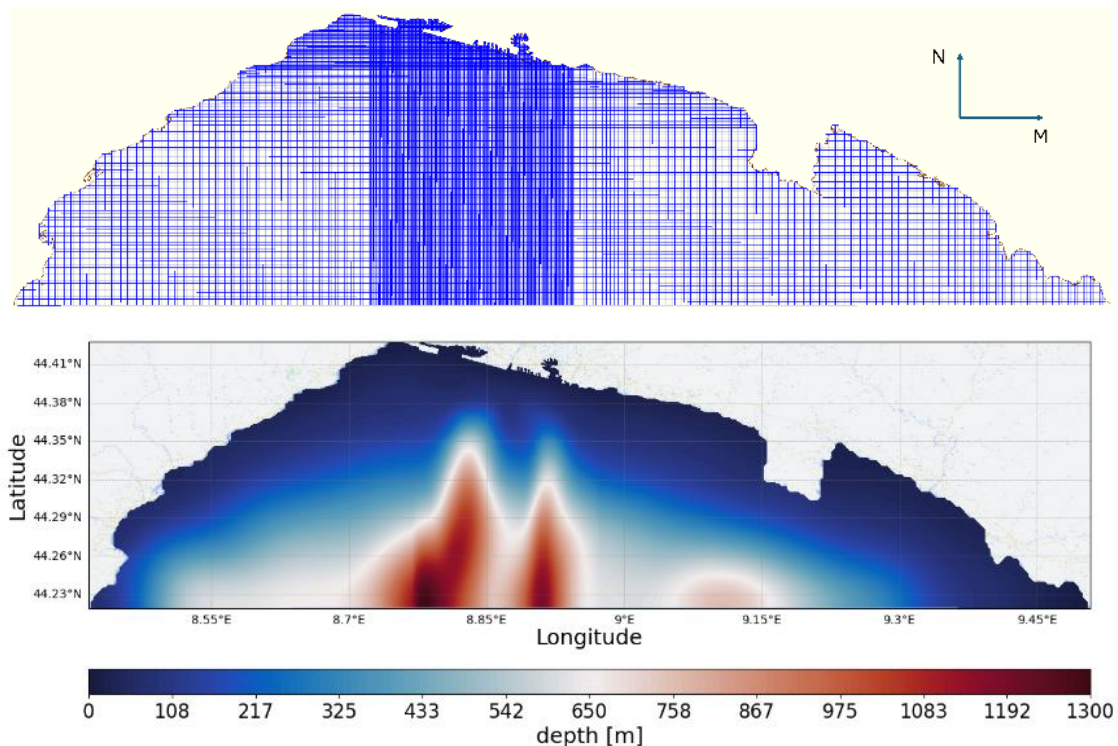


Figure 6 - On top: high resolution regular grid; down: bathymetry.

Scenarios selection

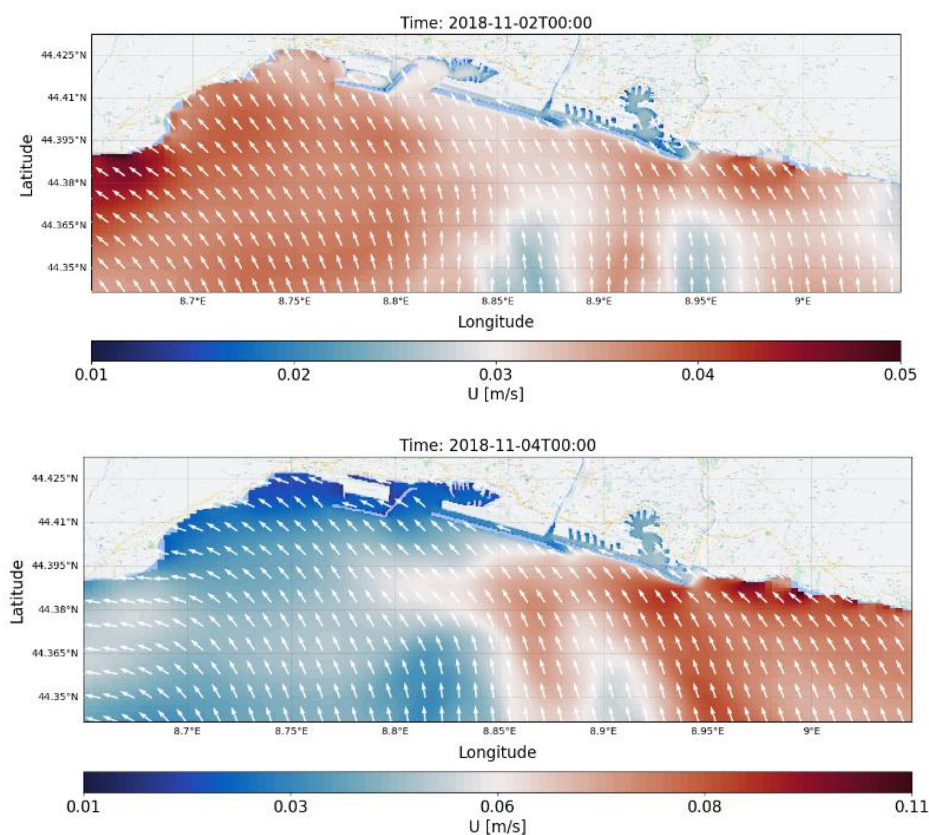
The environmental variables used to force the model are: wind, wave, tide and regional current. To account for the environmental variability in the domain, a 40-year dataset from the MeteOcean research group at the University of Genoa was analyzed. This dataset includes hourly wind and wave measurements across the Mediterranean Sea.

A systematic approach was used to identify key periods based on wave height. The dataset was scanned week by week, selecting weeks with significant wave events. These selected weeks were further classified based on wave energy, wind-wave interactions, directional variability, and predominant wave direction.

This process resulted in 23 representative scenarios, each capturing distinct oceanographic conditions. For each scenario, the most typical week was chosen. Additional data on large-scale currents and tides were incorporated to define the boundary conditions for hydrodynamic simulations. Tide and large-scale currents were gathered respectively from OSU TPXO model and Copernicus Marine Data Store.

Results

Once combined the aforementioned boundary conditions with the geographical information of the domain, the model can be run. The following figures represent an example of marine circulation in the Genoa port at various time intervals, for scenario 01.



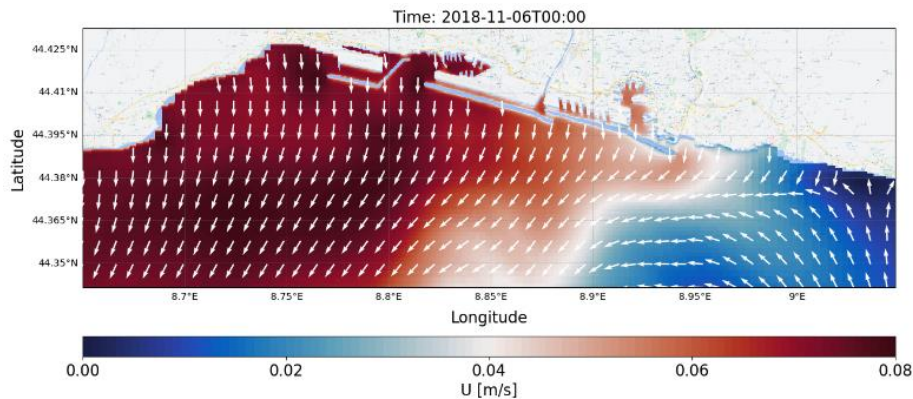


Figure 7 - Velocity field for scenario 01 at different time intervals, after 24, 72 and 120 hours from the initial time.

Model Validation

To assess the realism of the model outputs, water level measurements taken inside the port were used to validate the simulated current scenarios. The validation consists in comparing the model results with observed data through a variety of statistical methods, as shown in Figure 8. On the left side of the figure, the box plots summarize four commonly used indices:

1. **Normalized Root Mean Squared Error (NRMSE):** This statistic quantifies the average difference between model predictions and observations, normalized by the range of observed values. An NRMSE closer to zero indicates better model accuracy.
2. **Hanna-Heinold Statistic:** This statistic is another measure of model performance, designed for atmospheric models but applicable in other contexts. It should also tend toward zero when the model is well-calibrated against observations.
3. **Pearson Correlation Coefficient:** This is a measure of the linear relationship between model predictions and observations. A value of 1 indicates perfect correlation, meaning that the model captures the variability of the observed data accurately.
4. **SKILL Score:** This is a composite index that evaluates model performance by combining the correlation and error metrics. A SKILL score of 1 reflects a perfect model, while values close to zero indicate poor performance.

The box plots help visualize the distribution of each statistic across multiple time points or scenarios, highlighting the median, quartiles, and any potential outliers. The general trend shows favorable agreement between the model and the observations.

On the right side, a Taylor diagram provides a more comprehensive comparison between model outputs and observations, using three key statistics:

- **Pearson Correlation:** Reiterated here to show the linear correlation between the model and observations.
- **Root Mean Square Error (RMSE):** Visualized as the radial distance from the origin. Lower RMSE values, closer to the observed data point, indicate better model performance.
- **Standard Deviation:** Represented as the angle around the diagram, this indicates how well the model reproduces the variability seen in the observations.

In the Taylor diagram, the violet circle represents the observed data. Model results are displayed as diamonds, and the closer these diamonds are to the violet circle, the better the model's performance. Finally, the colors of the diamonds are in function of the bias in centimeters. The diagram confirms that the model performs well in reproducing the observed water levels, especially considering the complexity of the Gulf of Genoa's coastline and the numerous environmental variables influencing the currents.

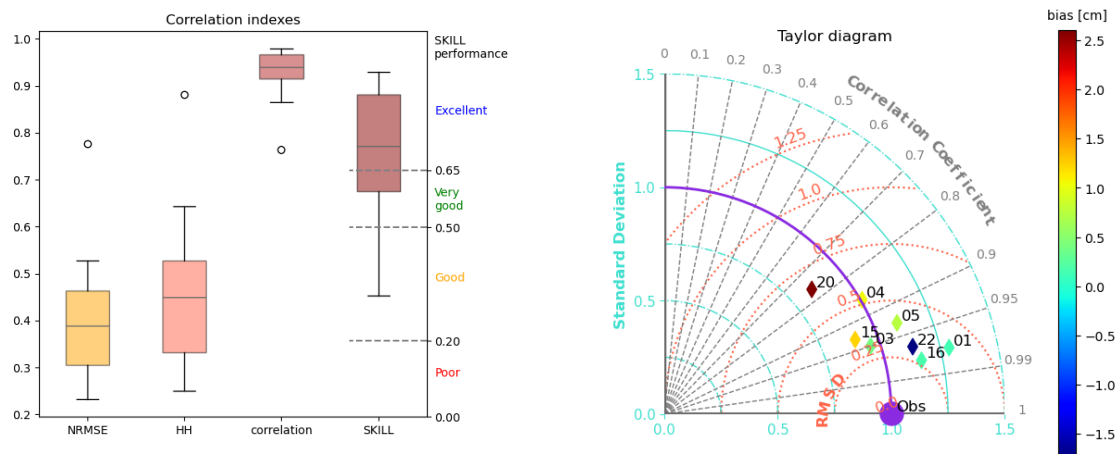


Figure 8 - Validation plots. On the left. Box plot of Normalized Root Mean Square Error, Hanna Heinold, Pearson Correlation, Skill coefficient; on the right: Taylor diagram.

The hydrodynamic modeling approach described above has been applied specifically to Genoa, as the hydrodynamics of Aqaba and Tripoli were already implemented in the Be-Ready project. However, in addition to ocean dynamics, atmospheric conditions play a crucial role in pollutant dispersion, particularly for very volatile substances.

2.2. Atmospheric modelling

Atmospheric modeling has been conducted for Aqaba and Tripoli, using the Weather Research and Forecasting (WRF) model, a widely adopted tool for weather prediction and research. Developed by institutions such as NCAR and NOAA, WRF provides high-resolution simulations, making it ideal for studying wind patterns and their influence on coastal hydrodynamics.

2.2.1. Model description

WRF is a non-hydrostatic numerical model designed for both research and operational forecasting. It allows for detailed representation of weather phenomena, from large-scale atmospheric circulation to small, localized systems. The model setup includes nested grids to refine resolution over key areas and a selection of physical parameterizations to capture atmospheric processes accurately.

Key Components:

- **Wind and Turbulence Representation:** The model accounts for wind dynamics, including turbulence near the surface, to ensure realistic air-sea interactions.
- **Microphysics and Radiation:** Different parameterizations help simulate cloud formation, precipitation, and energy exchanges between the atmosphere and ocean.
- **Boundary Layer Processes:** Surface-atmosphere exchanges of heat, moisture, and momentum are represented through land-surface models, ensuring accurate wind forcing on the hydrodynamic model.

2.2.2. Model application

Two specific domains were defined for the regions of Aqaba and Tripoli. These domains were selected based on the project's requirements to capture localized atmospheric conditions with high precision. For this purpose, high-resolution fields with a horizontal resolution of 1.1 km x 1.1 km were defined.

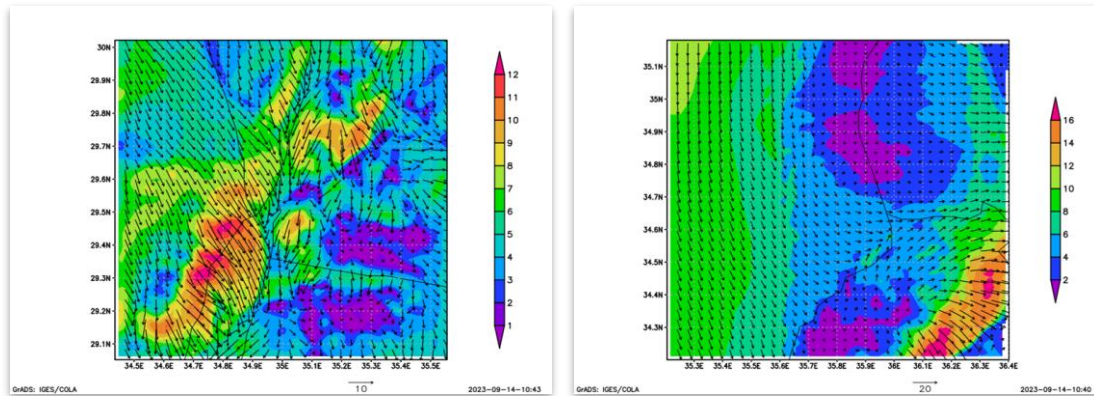


Figure 9 - Typical output of the atmospheric modelling

The downscaling of global weather forecast models to these high-resolution domains was achieved using a one-way nesting procedure, which allows for the integration of coarse global data into finer local domains. The nesting procedure was essential for refining large-scale meteorological data to capture the variability and detail required for local climate simulations.

Scenarios Selection and Simulation

The atmospheric simulations were carried out for a subset of possible scenarios, carefully chosen to represent the variability of the local climate. These scenarios were selected using big data analysis algorithms, which identified key time frames that needed to be downscaled. This strategic approach ensured that the simulations covered the range of atmospheric conditions that could influence pollutant behavior in the target regions. The WRF model was configured to run high-resolution simulations over these selected time frames, providing the necessary meteorological data for further pollutant dispersion modeling in the web platform.

Post-processing and Data Transformation

Following the atmospheric simulations, an intensive postprocessing phase was conducted to prepare the WRF model outputs for integration with the TESEO platform, which is the core of PROMPT DSS system. This phase involved several key steps to ensure that the data met the platform's specific requirements.

The WRF model output originally consisted of an ensemble of 2D to 10D matrices representing 117 different parameters. Each file contained one hour of meteorological data. However, only five of these parameters were considered relevant to the project objectives

and the TESEO platform. These key parameters, including wind speed, temperature, and humidity, were extracted and used to create the final output files. To meet the platform's requirements, the data were transformed from the WRF's native X-Y grid to a smaller latitude-longitude grid. This process involved reparametrizing the grid and applying interpolation techniques to reconcile any discrepancies between grid points.

The WRF outputs, initially available as hourly data files, were merged into a total of 50 final files, 25 for each region (Aqaba and Tripoli). Each file was structured to represent distinct atmospheric scenarios, as defined in the earlier stages of the project. For each location and scenario, 168 individual 2D fields were merged into 3D matrices, ensuring that the data were correctly aligned within the desired coordinate system and limited to the specific areas of interest. This approach allowed the project team to generate a compact, high-resolution dataset, tailored for integration with the TESEO platform for further analysis and visualization.

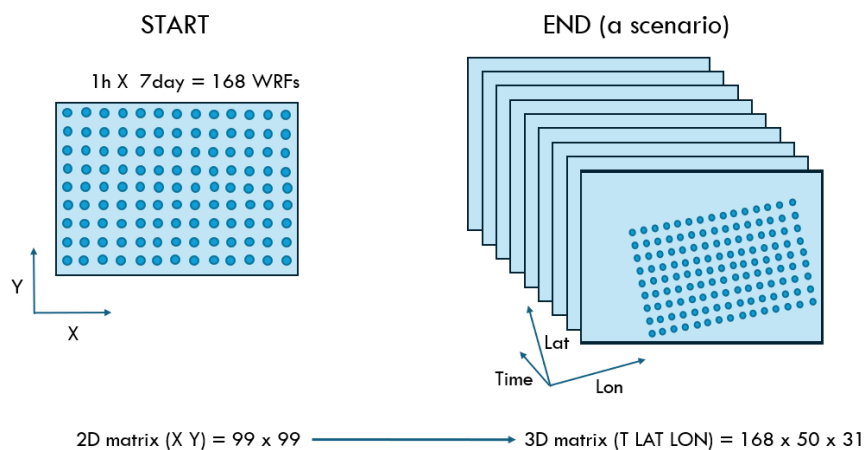


Figure 10 - Atmospheric output structure

3. POLLUTION MODELLING: MARINE AND ATMOSPHERIC

Understanding pollutant dispersion in both the marine and atmospheric environments is essential for assessing the potential impact of hazardous substances. In this project, two dedicated models have been used to simulate the transport and fate of pollutants: an oceanographic model for marine dispersion and an atmospheric model for air pollutant transport.

Marine pollutant dispersion is simulated using a Lagrangian particle tracking model, which allows for the detailed representation of pollutant advection, diffusion, and weathering processes within the hydrodynamic environment. This approach provides insights into how pollutants move and transform in the water column, helping to evaluate risks and optimize response strategies.

Atmospheric dispersion modeling, on the other hand, is crucial for assessing the transport of airborne pollutants, particularly in coastal regions where wind patterns influence both marine and atmospheric contamination. The Weather Research and Forecasting (WRF) model has been used to simulate atmospheric conditions, providing high-resolution data to support dispersion predictions.

The outputs of these models serve as key inputs for the risk assessment, which is presented in the chapter 4. While this section focuses on describing the model setup and methodology, the subsequent analysis will evaluate the implications of pollutant dispersion in each study site.

In the Decision Support System (DSS), described in chapter 5, users will have the capability to run marine pollutant dispersion simulations for all study sites (Genoa, La Spezia, Aqaba, and Tripoli). However, atmospheric dispersion simulations are available only for Aqaba and Tripoli, where dedicated atmospheric modeling has been performed.

3.1. Marine pollution modelling

Marine pollution modelling is calculated using TESEO numerical model developed by IHCantabria. This is a Lagrangian numerical model able to calculate the trajectories of a substance released at the sea and its weathering evolution.

During the project, Genoa study case has been implemented as a new site to provide oil and chemical modelling. While the sites of Aqaba, Tripoli and La Spezia are preserved on the system from the previous project Be-Ready and will remain fully functional as presented on Figure 5.

3.1.1. Model description (TESEO)

The spill forecast system is based on the state-of-the-art oil spill model called TESEO, developed by the Environmental Hydraulics Institute (IHCantabria) in the framework of several Spanish and European projects (Abascal et al., 2007; Abascal et al., 2017a; Chiri et al., 2020). The HNS forecast module is based on an adaptation of the model for chemical substances, carried out in the framework of SICMA project (<https://sicma.ihcantabria.es/en/>). The Be-Ready operational forecast system integrates both, oil and HNS spill numerical models in a unified version of the model for rapid response in case of accidental pollution.

Therefore, TESEO is a 3D numerical model to simulate the transport, weathering and spatial distribution of oil and HNS spills in the marine environment both at regional scale (offshore) and coastal scale (bays, estuaries and harbours). To achieve this objective the model consists of transport and a weathering module to represent the evolution of the spills in the marine environment. The transport module simulates the drift process of the spilled pollutant by tracking independent numerical particles equivalent to the slick. The evolution of the particles is computed by the superposition of the transport induced by wind, currents and/or waves and turbulent dispersion. The weathering module incorporates the spreading, evaporation, emulsification, dissolution, viscosity and density changes, dispersion in water column, sedimentation and adhesion to coast. TESEO has been calibrated and validated in several studies with drifters buoys (e.g. Sotillo et al., 2008; Abascal et al., 2017a,b).

3.1.1.1. Transport and Dispersion

The TESEO transport module simulates pollutant movement using a Lagrangian approach, where the spill is represented by numerical particles. Their motion is influenced by surface currents, wind, waves, and turbulent diffusion.

The model calculates transport as the combination of advective and diffusive velocities. Advection is driven by currents and wind forecasts, while diffusion is simulated using a Monte Carlo approach based on a diffusion coefficient.

In addition to diffusion, the model accounts for oil spreading, a process governed by mechanical forces such as gravity, inertia, viscosity, and surface tension. The model implements spreading calculations based on established methods, such as those by Fay (1971) for oil spills and Kolluru (1992) for hazardous and noxious substances (HNS). These approaches estimate the slick's expansion over time, considering factors like spill volume, fluid density, and viscosity

3.1.1.2. Weathering processes for Oil spills

Evaporation

Evaporation is a key weathering process, significantly reducing the amount of oil remaining in the environment. Light crude oils can lose up to 75% of their mass within a few days, while heavier oils may only evaporate up to 10%. The model estimates evaporation using an analytical approach, where the rate depends on environmental factors such as wind speed, temperature, and oil composition.

Emulsification

Emulsification occurs when oil mixes with water, forming stable water-in-oil emulsions that increase the volume of the spill and alter its properties. The TESEO model follows a widely used method to simulate this process, where water uptake is influenced by wind speed and oil type. The formation rate varies depending on the maximum water content the oil can absorb and its chemical characteristics.

Physicochemical properties

Over time, the physical and chemical properties of oil evolve due to weathering. The TESEO model accounts for changes in density and viscosity, which are influenced by evaporation, emulsification, and temperature variations. Oil viscosity tends to increase as it absorbs water and loses lighter components, while density changes depend on the amount of water mixed into the oil and the degree of evaporation. These transformations affect how the oil behaves in the environment, influencing its transport and cleanup strategies.

3.1.1.3. Weathering processes for HNS spills

Evaporation

TESEO model estimates evaporation following the approach of Kawamura and Mackay (1985) and Fernandes (2014). Evaporation is influenced by factors such as the surface area of the spill, wind speed, molecular weight, and vapor pressure of the chemical. The mass transfer coefficient, which governs the rate of evaporation, depends on wind speed, pool diameter, and the Schmidt number of the chemical. The Schmidt number itself is determined by the ratio of kinematic viscosity to molecular diffusivity, which can be estimated using Graham's Law.

To account for volatility, a correction factor is applied based on the relative values of atmospheric pressure and vapor pressure. This correction is particularly relevant for chemicals below their boiling point, adjusting the evaporation rate accordingly.

Dissolution

Dissolution represents the process where a chemical dissolves into water, affecting its dispersion and impact. The TESEO model calculates dissolution using the methodology from Mackay and Leinonen (1977) and Fernandes (2014). The amount of dissolved mass depends on factors such as the solubility of the chemical, the available surface area of the slick, and a mass transfer coefficient.

The mass transfer coefficient is influenced by the Sherwood number, which depends on the Schmidt and Reynolds numbers. The chemical's diffusivity in water is estimated using empirical correlations based on molecular weight and viscosity. The surface area of the slick and characteristic length of the spill are used to refine the dissolution estimates.

For surface slicks, the wind velocity plays a crucial role in determining the Reynolds number, which, combined with the Schmidt number, helps estimate dissolution rates. These factors contribute to understanding how quickly an HNS spill disperses in water, aiding response efforts and impact assessment.

3.1.2. Model implementation in each study case

The number of spill scenarios for oil (N_{SC-OIL}) and HNS (N_{SC-HNS}) is estimated based on the following steps: i) selection of the critical points or potential spill locations (N_P); ii) selection of oil products/chemical substances representative of each critical point (N_S) and iii) selection of representative spill volumes (N_V):

$$N_{SC-OIL} = N_P \times N_S \times N_V$$

$$N_{SC-HNS} = N_P \times N_S \times N_V$$

The oil and HNS spill scenarios for each pilot site are presented below:

Port of Genoa (implemented in Prompt)

The Figure 11 shows the oil spill positions selected (top panel), which reflect the areas of the port most affected by ship traffic, and the HNS spill positions selected (down panel), corresponding to the two docks where the chemicals deposit are located.

A total of 12 oil spill and 13 HNS spill scenarios have been selected, as described in Table 1 and Table 2, respectively.

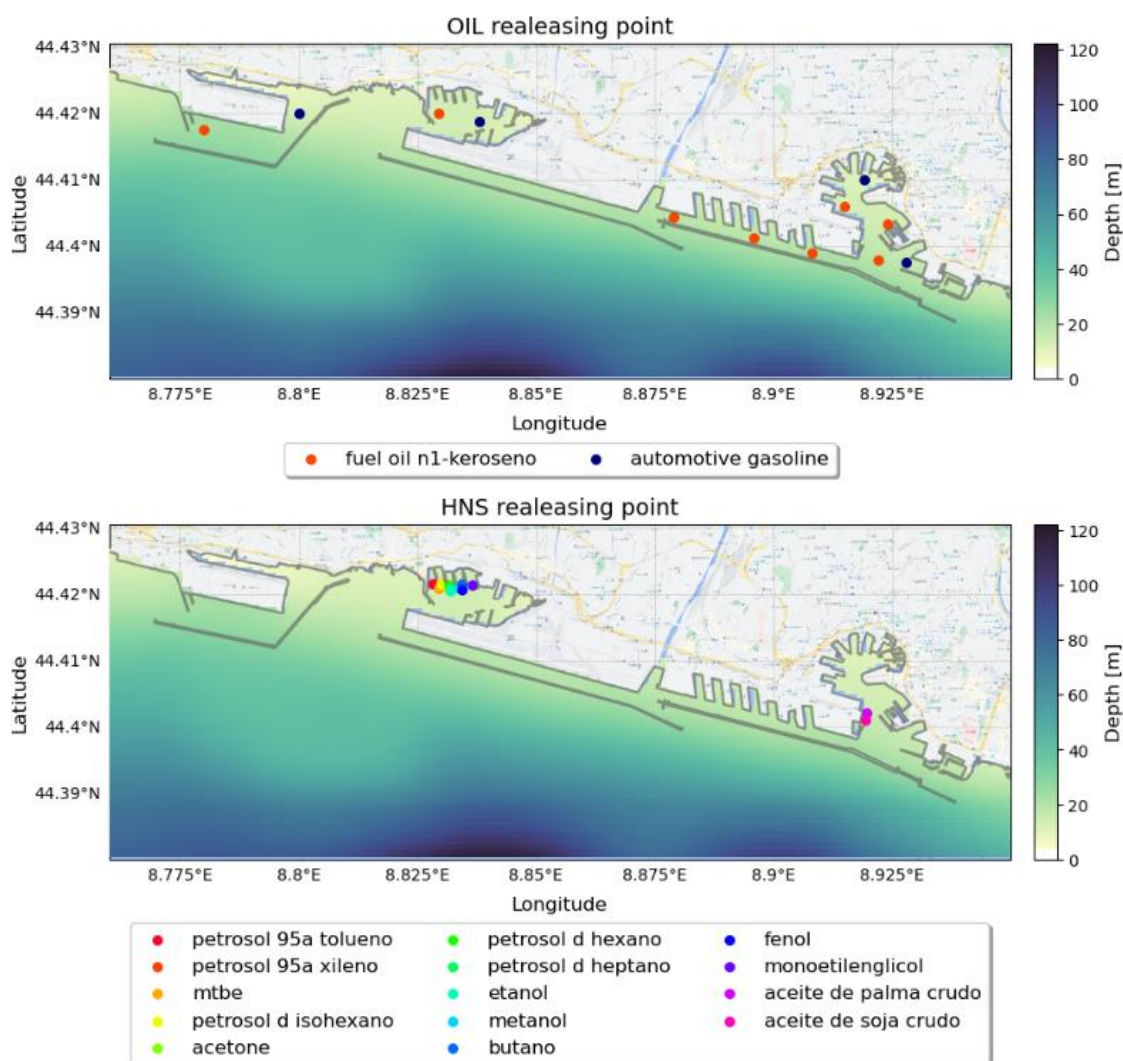


Figure 11 - Releasing positions for oil (top) and HNS (down) spills.

The oil characteristics for each spill point has been established considering the typical oil used as fuel by cargos and large cruises (fuel oil n1-keroseno) and by recreational boat (automotive gasoline). In Table 1 are shown the properties of these substances, which have been obtained from official sources including the National Centre for Biotechnology Information (NCBI, <https://pubchem.ncbi.nlm.nih.gov/>) and the European Chemicals Agency (ECHA, <https://echa.europa.eu/>). Based on this information, substances have been classified according to their behaviour into the following categories: F: floater; FE: floater/evaporator.

Table 1 - Oil spill points in Genoa.

Terminal	lat	lon	Substance	Type	Volume (m ³)	Behavior	In Teseo (Y/N)	Terminal type
Prà	44,4177	8,78	fuel oil n1-keroseno	Oil	5	FE	Y	channel
Prà	44,42	8,8	automotive gasoline	Oil	5	F	Y	channel
Multedo	44,42	8,8295	fuel oil n1-keroseno	Oil	5	FE	Y	channel
Multedo	44,4189	8,838	automotive gasoline	Oil	5	F	Y	channel
Sampierdarena	44,4044	8,879	fuel oil n1-keroseno	Oil	5	FE	Y	channel
Sampierdarena	44,4013	8,8958	fuel oil n1-keroseno	Oil	5	FE	Y	channel
Sampierdarena	44,39905	8,908	fuel oil n1-keroseno	Oil	5	FE	Y	channel
Porto Antico	44,398	8,922	fuel oil n1-keroseno	Oil	5	FE	Y	manouvering area
Porto Antico	44	9	automotive gasoline	Oil	5	F	Y	Manouvering area
Porto Antico	44	8,9239	fuel oil n1-keroseno	Oil	5	FE	Y	dry dock
Porto Antico	44,406	8,915	fuel oil n1-keroseno	Oil	5	FE	Y	porto antico basin
Porto Antico	44,41	8,9192	automotive gasoline	Oil	5	F	Y	porto antico basin

The HNS characteristics for each spill point have been established based on the chemical substances managed in the two chemical deposit in the Port of Genoa, according to the documents provided by the chemical companies, through their websites. In Table 2 **Errore. L'origine riferimento non è stata trovata.** are shown the properties of these substances, which have been obtained from official sources including the National Center for Biotechnology Information (NCBI, <https://pubchem.ncbi.nlm.nih.gov/>) and the European Chemicals Agency (ECHA, <https://echa.europa.eu/>). Based on this information, substances have been classified according to their behaviour into the following categories: G: gas; D: dissolver; E: *evaporator*; F: *floaters*; S: *sinker*; DE: *dissolver/evaporator*; ED: *evaporator/dissolver*; FD: *floaters/dissolver*; FE: *floaters/evaporator*; SD: *sinker/dissolver*.

Table 2 - HNS spill points in Genoa.

Terminal	lat	lon	Substance in terminal	Substance	Formula	Volume (m ³)	Behavior	Terminal type
Multedo	44, 42	8,82834	toluene	petrosol 95a tolueno	C ₇ H ₈	5	FE	deposit of chemicals
Multedo	44, 42	8,82998	xylene	petrosol 95a xileno	C ₈ H ₁₀	5	E	deposit of chemicals
Multedo	44, 42	8,8294	methyl ethyl ketone	mtbe	C ₅ H ₁₂ O	5	SD	deposit of chemicals
Multedo	44, 42	8,82988	methoxypropyl acetate	petrosol d isohecano	C ₆ H ₁₂ O ₃	5	E	deposit of chemicals
Multedo	44, 42	8,83165	acetone	acetone	C ₃ H ₆ O	5	SD	deposit of chemicals
Multedo	44, 42	8,83172	hexane	petrosol d hexano	C ₆ H ₁₄	5	E	deposit of chemicals
Multedo	44, 42	8,8324	heptane	petrosol d heptano	C ₇ H ₁₆	5	E	deposit of chemicals
Multedo	44, 42	8,832	ethanol	etanol	C ₂ H ₆ O	5	D	deposit of chemicals
Multedo	44, 42	8,833799	methanol	metanol	CH ₄ O	5	D	deposit of chemicals
Multedo	44, 42	8,834284	dinitrophenol	fenol	C ₆ H ₆ O	5	SD	deposit of chemicals
Multedo	44, 42	8,8365	ethylene glycol	monoetile nglicol	C ₂ H ₆ O ₂	5	SD	deposit of chemicals
Bettolo	44	8,919624	palm oil	aceite de palma crudo	-	5	F	oil terminal
Bettolo	44	8,919399	soy oil	aceite de soja crudo	C ₁₁ H ₉ N ₃ O ₂ Na	5	F	oil terminal

Port of Tripoli (based on Be-Ready project)

According to Be-Ready results, the spill location of the scenarios selected in the Port of Tripoli are the following (see Figure 12):

- 1 point next to the ferry to Turkey station
- 1 point in the small boats and fish market port
- 3 points in the main port and 1 point in the entrance to the port
- 1 point next to the container terminal
- 1 point where the port expansion is projected (east of the container terminal)

- 4 points in the navigation areas with greater marine traffic
- 3 points in the ship waiting areas
- 1 point next to the International Petroleum Company (highlighted as a possible spill source)

A total of 30 oil spill and 44 HNS spill scenarios has been selected (combination of the aforementioned locations, products and volume), as described in Table 3 and Table 4, respectively.

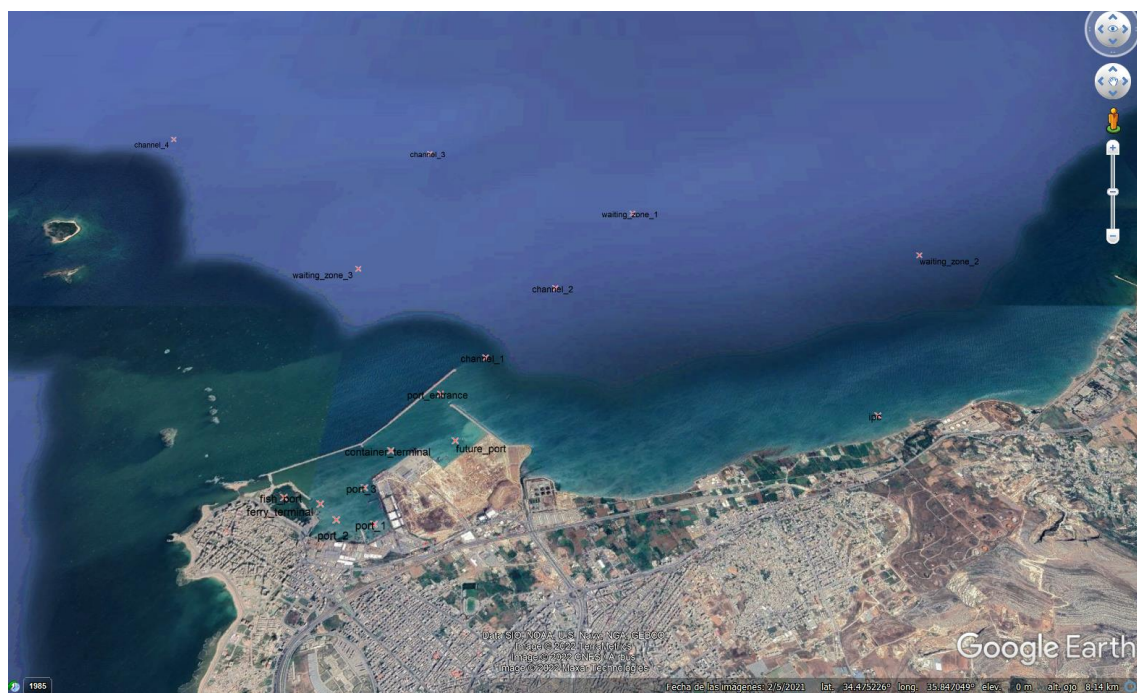


Figure 12 - Location of the spill points in the Port of Tripoli.

Table 3 - Oil spill scenarios selected in the Port of Tripoli.

SpillNo.	Point	Ref.	Lat.	Long.	Substance	Type	Volume [m ³]
1	ferry_terminal	Tasucu Ferry Terminal	35°49'12"	34°27'17"	Fuel Oil N1-Keroseno	1	5
2	fish_port	Al Mina Fish Port	35°48'55"	34°27'19"	Automotive Gasoline	1	5
3	fish_port	Al Mina Fish Port	35°48'55"	34°27'19"	Fuel Oil n1-Diesel	1	5
4	port_1	Main Port Southeast	35°49'33"	34°27'08"	Fuel Oil N1-Keroseno	1	5
5	port_1	Main Port Southeast	35°49'33"	34°27'08"	Fuel Oil n6	1	5
6	port_2	Main Port Southwest	35°49'18"	34°27'09"	Fuel Oil N1-Keroseno	1	5
7	port_2	Main Port Southwest	35°49'18"	34°27'09"	Fuel Oil n6	1	5
8	port_3	Main Port North	35°49'27"	34°27'23"	Fuel Oil N1-Keroseno	1	5
9	port_3	Main Port North	35°49'27"	34°27'23"	Fuel Oil n6	1	5
10	container_terminal	Main Port Container Terminal	35°49'35"	34°27'38"	Fuel Oil N1-Keroseno	1	5
11	port_entrance	Main Port Entrance	35°49'52"	34°28'04"	Fuel Oil N1-Keroseno	1	5
12	port_entrance	Main Port Entrance	35°49'52"	34°28'04"	Fuel Oil n6	1	5
13	future_port	Main Port Expansion Zone	35°50'01"	34°27'42"	Fuel Oil N1-Keroseno	1	5
14	future_port	Main Port Expansion Zone	35°50'01"	34°27'42"	Fuel Oil n6	1	5
15	channel_1	Channel South	35°50'11"	34°28'22"	Fuel Oil N1-Keroseno	1	5
16	channel_1	Channel South	35°50'11"	34°28'22"	Fuel Oil n6	1	5
17	channel_2	Channel Center-South	35°50'42"	34°29'01"	Fuel Oil N1-Keroseno	1	5
18	channel_2	Channel Center-South	35°50'42"	34°29'01"	Fuel Oil n6	1	5
19	waiting_zone_1	Waiting Zone Center	35°51'21"	34°29'48"	Fuel Oil N1-Keroseno	1	5
20	waiting_zone_1	Waiting Zone Center	35°51'21"	34°29'48"	Fuel Oil n6	1	5
21	channel_3	Channel Center-North	35°49'28"	34°30'31"	Fuel Oil N1-Keroseno	1	5
22	channel_3	Channel Center-North	35°49'28"	34°30'31"	Fuel Oil n6	1	5
23	channel_4	Channel Northwest	35°47'00"	34°30'43"	Fuel Oil N1-Keroseno	1	5
24	channel_4	Channel Northwest	35°47'00"	34°30'43"	Fuel Oil n6	1	5
25	waiting_zone_2	Waiting Zone East	35°53'42"	34°29'19"	Fuel Oil N1-Keroseno	1	5
26	waiting_zone_2	Waiting Zone East	35°53'42"	34°29'19"	Fuel Oil n6	1	5
27	waiting_zone_3	Waiting Zone West	35°49'03"	34°29'12"	Fuel Oil N1-Keroseno	1	5
28	waiting_zone_3	Waiting Zone West	35°49'03"	34°29'12"	Fuel Oil n6	1	5
29	ipc	International Petroleum Company	35°52'57"	34°27'53"	Arabian Light	0	5
30	ipc	International Petroleum Company	35°52'57"	34°27'53"	Fuel Oil n6	1	5

Table 4 - HNS spill scenarios selected in the Port of Tripoli.

Spill no.	Point	Ref.	Lat.	Long.	Substance	SEBC	Volume (m ³)
1	port_1	Main Port Southeast	35°49'33"	34°27'08"	Etanol	D	5
2	port_1	Main Port Southeast	35°49'33"	34°27'08"	Benceno	E	5
3	port_1	Main Port Southeast	35°49'33"	34°27'08"	Cumeno	FE	5
4	port_1	Main Port Southeast	35°49'33"	34°27'08"	Fenol	SD	5
5	port_2	Main Port Southwest	35°49'18"	34°27'09"	Etanol	D	5
6	port_2	Main Port Southwest	35°49'18"	34°27'09"	Benceno	E	5
7	port_2	Main Port Southwest	35°49'18"	34°27'09"	Cumeno	FE	5
8	port_2	Main Port Southwest	35°49'18"	34°27'09"	Fenol	SD	5
9	port_3	Main Port North	35°49'27"	34°27'23"	Etanol	D	5
10	port_3	Main Port North	35°49'27"	34°27'23"	Benceno	E	5
11	port_3	Main Port North	35°49'27"	34°27'23"	Cumeno	FE	5
12	port_3	Main Port North	35°49'27"	34°27'23"	Fenol	SD	5
13	port_entrance	Main Port Entrance	35°49'52"	34°28'04"	Etanol	D	5
14	port_entrance	Main Port Entrance	35°49'52"	34°28'04"	Benceno	E	5
15	port_entrance	Main Port Entrance	35°49'52"	34°28'04"	Cumeno	FE	5
16	port_entrance	Main Port Entrance	35°49'52"	34°28'04"	Fenol	SD	5
17	channel_1	Channel South	35°50'11"	34°28'22"	Etanol	D	5
18	channel_1	Channel South	35°50'11"	34°28'22"	Benceno	E	5
19	channel_1	Channel South	35°50'11"	34°28'22"	Cumeno	FE	5
20	channel_1	Channel South	35°50'11"	34°28'22"	Fenol	SD	5
21	channel_2	Channel Center South	35°50'42"	34°29'01"	Etanol	D	5
22	channel_2	Channel Center South	35°50'42"	34°29'01"	Benceno	E	5
23	channel_2	Channel Center South	35°50'42"	34°29'01"	Cumeno	FE	5
24	channel_2	Channel Center South	35°50'42"	34°29'01"	Fenol	SD	5
25	waiting_zone_1	Waiting Zone Center	35°51'21"	34°29'48"	Etanol	D	5
26	waiting_zone_1	Waiting Zone Center	35°51'21"	34°29'48"	Benceno	E	5
27	waiting_zone_1	Waiting Zone Center	35°51'21"	34°29'48"	Cumeno	FE	5
28	waiting_zone_1	Waiting Zone Center	35°51'21"	34°29'48"	Fenol	SD	5
29	channel_3	Channel Center North	35°49'28"	34°30'31"	Etanol	D	5
30	channel_3	Channel Center North	35°49'28"	34°30'31"	Benceno	E	5
31	channel_3	Channel Center North	35°49'28"	34°30'31"	Cumeno	FE	5
32	channel_3	Channel Center North	35°49'28"	34°30'31"	Fenol	SD	5
33	channel_4	Channel Northwest	35°47'00"	34°30'43"	Etanol	D	5
34	channel_4	Channel Northwest	35°47'00"	34°30'43"	Benceno	E	5
35	channel_4	Channel Northwest	35°47'00"	34°30'43"	Cumeno	FE	5
36	channel_4	Channel Northwest	35°47'00"	34°30'43"	Fenol	SD	5
37	waiting_zone_2	Waiting Zone East	35°53'42"	34°29'19"	Etanol	D	5
38	waiting_zone_2	Waiting Zone East	35°53'42"	34°29'19"	Benceno	E	5
39	waiting_zone_2	Waiting Zone East	35°53'42"	34°29'19"	Cumeno	FE	5
40	waiting_zone_2	Waiting Zone East	35°53'42"	34°29'19"	Fenol	SD	5
41	waiting_zone_3	Waiting Zone West	35°49'03"	34°29'12"	Etanol	D	5
42	waiting_zone_3	Waiting Zone West	35°49'03"	34°29'12"	Benceno	E	5
43	waiting_zone_3	Waiting Zone West	35°49'03"	34°29'12"	Cumeno	FE	5
44	waiting_zone_3	Waiting Zone West	35°49'03"	34°29'12"	Fenol	SD	5

Port of Aqaba (based on Be-Ready project)

According to Be-Ready results, the spill location of the scenarios selected in the Port of Aqaba are the following (see Figure 13):

- 1 point next to the main leisure port and 1 point next to the fish market port.
- 3 points in the main port (north port).
- 2 points in the middle port and 1 point in the ferry terminal right next to it to the south.
- 1 point in the Naval Base.
- 1 point in each of the industrial port terminals.

- 2 points in the new port.
- 4 points in the navigation areas with greater marine traffic.

A total of 29 oil spill and 32 HNS spill scenarios has been selected (combination of the aforementioned locations, products and volume), as described in Table 5 and Table 6, respectively.



Figure 13 - Location of the spill points in the Port of Aqaba.

Table 5 - Oil spill scenarios selected in the Port of Aqaba.

Spill no.	Point	Ref.	Lat.	Long.	Substance	Type	Volume [m ³]	Dens. [kg/m ³]	Mass [kg]
1	leisure_port	Royal Yacht Club	29°31'45.30"N	34°59'49.60"E	Automotive Gasoline	1	5	742	3710
2	leisure_port	Royal Yacht Club	29°31'45.30"N	34°59'49.60"E	Fuel Oil n1-Diesel	1	5	834	4170
3	fishing_port	Fish Market Port	29°31'13.39"N	34°59'56.52"E	Automotive Gasoline	1	5	742	3710
4	fishing_port	Fish Market Port	29°31'13.39"N	34°59'56.52"E	Fuel Oil n1-Diesel	1	5	834	4170
5	main_port_1	Main Port North	29°31'3.90"N	34°59'55.04"E	Light refined oil (Fuel Oil N1-Keroseno)	1	5	816	4080
6	main_port_2	Main Port Center	29°30'51.48"N	34°59'40.87"E	Light refined oil (Fuel Oil N1-Keroseno)	1	5	816	4080
7	main_port_3	Main Port South	29°30'20.76"N	34°59'29.47"E	Light refined oil (Fuel Oil N1-Keroseno)	1	5	816	4080
8	mid_port_1	Middle Port North	29°28'47.48"N	34°58'46.97"E	Light refined oil (Fuel Oil N1-Keroseno)	1	5	816	4080
9	mid_port_2	Middle Port South	29°28'5.23"N	34°58'26.11"E	Light refined oil (Fuel Oil N1-Keroseno)	1	5	816	4080
10	ferry_terminal	Middle Port Ferry Terminal	29°27'39.34"N	34°58'25.88"E	Light refined oil (Fuel Oil N1-Keroseno)	1	5	816	4080
11	naval_base	Royal Jordanian Naval Base	29°23'39.88"N	34°57'47.46"E	Automotive Gasoline	1	5	742	3710
12	naval_base	Royal Jordanian Naval Base	29°23'39.88"N	34°57'47.46"E	Fuel Oil n1-Diesel	1	5	834	4170
13	naval_base	Royal Jordanian Naval Base	29°23'39.88"N	34°57'47.46"E	Light refined oil (Fuel Oil N1-Keroseno)	1	5	816	4080
14	lpg_terminal	Liquefied Petroleum Gas Terminal	29°23'8.27"N	34°57'53.66"E	Light refined oil (Fuel Oil N1-Keroseno)	1	5	816	4080
15	oil_terminal	Oil Terminal	29°22'57.81"N	34°57'46.25"E	Crude oil (Arabian Light)	0	5	869	4345
16	oil_terminal	Oil Terminal	29°22'57.81"N	34°57'46.25"E	Heavy refined oil (Fuel Oil n6)	1	5	979	4895
17	lng_terminal	Liquefied Natural Gas Terminal	29°22'30.36"N	34°57'40.28"E	Light refined oil (Fuel Oil N1-Keroseno)	1	5	816	4080
18	jipc_terminal	Industrial Terminal	29°22'9.83"N	34°57'32.22"E	Heavy refined oil (Fuel Oil n6)	1	5	979	4895
19	jipc_terminal	Industrial Terminal	29°22'9.83"N	34°57'32.22"E	Light refined oil (Fuel Oil N1-Keroseno)	1	5	816	4080
20	new_port_1	New Port North	29°21'48.11"N	34°57'38.93"E	Light refined oil (Fuel Oil N1-Keroseno)	1	5	816	4080
21	new_port_2	New Port South	29°21'39.36"N	34°57'49.76"E	Light refined oil (Fuel Oil N1-Keroseno)	1	5	816	4080
22	channel_1	Channel South	29°23'3.68"N	34°54'4.13"E	Light refined oil (Fuel Oil N1-Keroseno)	1	5	816	4080
23	channel_1	Channel South	29°23'3.68"N	34°54'4.13"E	Heavy refined oil (Fuel Oil n6)	1	5	979	4895
24	channel_2	Channel Center-South	29°25'50.04"N	34°56'0.58"E	Light refined oil (Fuel Oil N1-Keroseno)	1	5	816	4080
25	channel_2	Channel Center-South	29°25'50.04"N	34°56'0.58"E	Heavy refined oil (Fuel Oil n6)	1	5	979	4895
26	channel_3	Channel Center-North	29°28'36.12"N	34°57'36.10"E	Light refined oil (Fuel Oil N1-Keroseno)	1	5	816	4080
27	channel_3	Channel Center-North	29°28'36.12"N	34°57'36.10"E	Heavy refined oil (Fuel Oil n6)	1	5	979	4895
28	channel_4	Channel North	29°30'42.29"N	34°58'53.57"E	Light refined oil (Fuel Oil N1-Keroseno)	1	5	816	4080
29	channel_4	Channel North	29°30'42.29"N	34°58'53.57"E	Heavy refined oil (Fuel Oil n6)	1	5	979	4895

Table 6 - HNS spill scenarios selected in the Port of Aqaba.

SpillNo.	Point	Ref.	Lat.	Long.	Substance	SEBC	Volume [m³]	Dens. [kg/m³]	Mass [kg]
1	main_port_3	Main Port South	29°30'20.76"N	34°59'29.47"E	Etanol	D	5	789,3	3946,5
2	main_port_3	Main Port South	29°30'20.76"N	34°59'29.47"E	Benceno	E	5	879,4	4397
3	main_port_3	Main Port South	29°30'20.76"N	34°59'29.47"E	Cumeno	FE	5	864	4320
4	main_port_3	Main Port South	29°30'20.76"N	34°59'29.47"E	Fenol	SD	5	1071	5355
5	mid_port_1	Middle Port North	29°28'47.48"N	34°58'46.97"E	Etanol	D	5	789,3	3946,5
6	mid_port_1	Middle Port North	29°28'47.48"N	34°58'46.97"E	Benceno	E	5	879,4	4397
7	mid_port_1	Middle Port North	29°28'47.48"N	34°58'46.97"E	Cumeno	FE	5	864	4320
8	mid_port_1	Middle Port North	29°28'47.48"N	34°58'46.97"E	Fenol	SD	5	1071	5355
9	jipc_terminal	Industrial Terminal	29°22'9.83"N	34°57'32.22"E	Etanol	D	5	789,3	3946,5
10	jipc_terminal	Industrial Terminal	29°22'9.83"N	34°57'32.22"E	Benceno	E	5	879,4	4397
11	jipc_terminal	Industrial Terminal	29°22'9.83"N	34°57'32.22"E	Cumeno	FE	5	864	4320
12	jipc_terminal	Industrial Terminal	29°22'9.83"N	34°57'32.22"E	Fenol	SD	5	1071	5355
13	new_port_2	New Port South	29°21'39.36"N	34°57'49.76"E	Etanol	D	5	789,3	3946,5
14	new_port_2	New Port South	29°21'39.36"N	34°57'49.76"E	Benceno	E	5	879,4	4397
15	new_port_2	New Port South	29°21'39.36"N	34°57'49.76"E	Cumeno	FE	5	864	4320
16	new_port_2	New Port South	29°21'39.36"N	34°57'49.76"E	Fenol	SD	5	1071	5355
17	channel_1	Channel South	29°23'3.68"N	34°54'4.13"E	Etanol	D	5	789,3	3946,5
18	channel_1	Channel South	29°23'3.68"N	34°54'4.13"E	Benceno	E	5	879,4	4397
19	channel_1	Channel South	29°23'3.68"N	34°54'4.13"E	Cumeno	FE	5	864	4320
20	channel_1	Channel South	29°23'3.68"N	34°54'4.13"E	Fenol	SD	5	1071	5355
21	channel_2	Channel Center-South	29°25'50.04"N	34°56'0.58"E	Etanol	D	5	789,3	3946,5
22	channel_2	Channel Center-South	29°25'50.04"N	34°56'0.58"E	Benceno	E	5	879,4	4397
23	channel_2	Channel Center-South	29°25'50.04"N	34°56'0.58"E	Cumeno	FE	5	864	4320
24	channel_2	Channel Center-South	29°25'50.04"N	34°56'0.58"E	Fenol	SD	5	1071	5355
25	channel_3	Channel Center-North	29°28'36.12"N	34°57'36.10"E	Etanol	D	5	789,3	3946,5
26	channel_3	Channel Center-North	29°28'36.12"N	34°57'36.10"E	Benceno	E	5	879,4	4397
27	channel_3	Channel Center-North	29°28'36.12"N	34°57'36.10"E	Cumeno	FE	5	864	4320
28	channel_3	Channel Center-North	29°28'36.12"N	34°57'36.10"E	Fenol	SD	5	1071	5355
29	channel_4	Channel North	29°30'42.29"N	34°58'53.57"E	Etanol	D	5	789,3	3946,5
30	channel_4	Channel North	29°30'42.29"N	34°58'53.57"E	Benceno	E	5	879,4	4397
31	channel_4	Channel North	29°30'42.29"N	34°58'53.57"E	Cumeno	FE	5	864	4320
32	channel_4	Channel North	29°30'42.29"N	34°58'53.57"E	Fenol	SD	5	1071	5355

3.2. Atmospheric pollution modelling

The project involved conducting atmospheric dispersion simulations using the HYSPLIT (Hybrid Single-Particle Lagrangian Integrated Trajectory) model. HYSPLIT, developed by NOAA, is widely used for simulating the transport and dispersion of airborne particles and pollutants, making it an ideal tool for this phase of the project.

3.2.1. Model description

HYSPLIT (Hybrid Single-Particle Lagrangian Integrated Trajectory) is one of the most widely used atmospheric dispersion and trajectory models in the world. Developed and maintained by NOAA's Air Resources Laboratory (ARL), HYSPLIT has become a standard tool for simulating the transport, dispersion, deposition, and chemical transformation of

pollutants, particles, and gases in the atmosphere. Its flexible and user-friendly nature allows for a wide range of applications, from forecasting air pollution events to studying long-range transport of atmospheric contaminants.

HYSPLIT is a hybrid model, combining **Lagrangian** and **Eulerian** approaches to provide high accuracy in tracking and predicting the dispersion of particles in the atmosphere. The model can compute the trajectories of individual air parcels (Lagrangian approach) or simulate the spread of pollutant concentrations on a grid (Eulerian approach), depending on the user's needs. This hybrid capability makes HYSPLIT highly versatile and capable of handling a wide range of atmospheric dispersion problems.

Key features of the HYSPLIT model include:

1. **Hybrid Modeling Approach:** HYSPLIT's core strength is its ability to simulate both the trajectory of particles as they move through the atmosphere and their dispersion across a grid, offering flexibility for different types of atmospheric studies.
2. **Pollutant Transport and Dispersion:** HYSPLIT tracks the transport of pollutants through the atmosphere based on meteorological data, simulating how particles or gases are carried by winds, deposited, or chemically transformed during their travel.
3. **Deposition and Wet Scavenging:** The model includes mechanisms for **dry deposition** (where pollutants settle on surfaces) and **wet deposition** (where pollutants are removed from the atmosphere by precipitation). This is crucial for studying the environmental impacts of contaminants.
4. **Backward and Forward Trajectories:** The model can compute both forward and backward trajectories. Forward trajectories predict the movement of pollutants or particles from a specific source, while backward trajectories can help trace the origin of pollutants observed at a specific location.

The performance and accuracy of HYSPLIT depend largely on the quality of the meteorological input data used to drive the model. HYSPLIT typically requires meteorological data that include 3D wind fields, temperature, humidity, and other variables that influence particle movement and atmospheric mixing.

3.2.2. Model implementation

HYSPLIT was configured to simulate pollutant dispersion in both the Aqaba and Tripoli regions. The setup involved specifying the emission sources, pollutant types, and release points based on the scenarios identified in the project. This configuration ensured that the

model accurately represented the behavior of pollutants under different atmospheric conditions. Key configuration steps included:

- Defining Emission Scenarios: Various pollutant emission scenarios were modeled, reflecting both natural and anthropogenic sources.
- Meteorological Forcing: The ARL files generated from WRF provided the meteorological inputs necessary to simulate how pollutants would be transported and dispersed by the wind, turbulence, and other atmospheric processes.

Generation of Meteorological Input Files

To drive the HYSPLIT simulations, it was necessary to convert the WRF outputs into a format compatible with the HYSPLIT model. This was achieved using NOAA's arw2arl preprocessor, which converts WRF-ARW outputs (in NetCDF format) into ARL (Air Resources Laboratory) files. These files contained the meteorological variables needed to run the HYSPLIT simulations, including wind fields and temperature. The ARL files played a pivotal role in integrating high-resolution meteorological data from WRF into the HYSPLIT model, ensuring accurate atmospheric dispersion simulations under the predefined scenarios.

Simulation Runs and Postprocessing

Multiple HYSPLIT simulations were executed for each meteorological scenario, using different pollutants and emission levels in line with IH Cantabria's data, generating detailed concentration and deposition maps that showed how pollutants dispersed over time within the target regions. These outputs were then postprocessed according to the TESEO platform's specifications, ensuring that the results were compatible for further analysis.

3.2.2.1. Coupling between TESEO and HYSPLIT

The results of TESEO simulations provide the necessary data to feed HYSPLIT emission source points. This coupling between the models has been made based on the following variables:

- The temporal evolution of the centre of mass of the oil slick
- The temporal evolution of the mass evaporated from the slick to the atmosphere
- The temporal evolution of the slick area

Based on these three variables, a postprocessing has been developed to generate an EMITIME file (emissions file) for the HYSPLIT model. This allows the definition of a source



point of emission with a specific area that can vary its location, area and mass emission ratio in time. Thus, the behaviour of the emission derived from a slick can be characterized and the produced evaporation of chemicals can be simulated considering the variability of the source, in this case, a slick that varies its area, location and ratio of mass emission in time.



4. RISK ASSESSMENT METHODOLOGY

One of the objectives of PROMPT is to develop a Risk Assessment Model for oil spills in marine environments and for HNS spills in marine and atmospheric environments. The Risk Assessment Model will support the response planning, providing the hazard, vulnerability and risk of the environment to oil and HNS spills in terms of probability. In other words, the risk assessment system will help planes and decision-makers answer many important planning questions such as:

Where may take place the potential spills?

What are the most likely places to be affected by a spill?

How long will a spill to reach a location?

What areas have to be protection priorities?

Risk is assumed to be made of hazard and vulnerability (i.e. $\text{Risk} = \text{Hazard} \times \text{Vulnerability}$). Hazard is defined as the probability of the coast and the marine/atmospheric environments (in particular, sensitive areas) to be polluted by an oil or HNS spill and is calculated in probabilistic terms. On the other hand, vulnerability is the environment's ability to cope with, resist and recover from the impact of pollution. Therefore, in order to develop a risk assessment model, both hazard and vulnerability has to be determined for oil in marine environment and for HNS spills in marine and atmospheric environments.

Figure 14 shows a general overview of the risk assessment model. The main steps of the methodology proposed are as follows:

- 1) Hazard analysis for oil and HNS spills. The hazard analysis is based on the following steps: i) selection of N oil and HNS spill scenarios (e.g. type of substance, spill point, spill release volume) according to the uses and activities in the different pilot sites; ii) selection of M met-ocean scenarios statistically representative of the pilot sites and obtained according to the methodology described in section 2; iii) numerical modelling ($M \times N$ simulations) of the spill evolution in the marine environment using the aforementioned TESEO model and in the atmosphere using the coupling between TESEO and HYSPLIT models; iv) statistical analysis of the results to obtain the probability maps of pollution and the arrival time of the pollutant to the potential affected areas.
- 2) Vulnerability assessment for oil and HNS spills. The methodology developed in Be-Ready is applied for marine pollution and adapted for atmospheric pollution. Both methodologies integrate different indexes considering the main physical, biological and/or socio-economical

characteristics, as well as the characteristics of the pollutants. As a result, vulnerability maps for the different indexes will be defined for oil spills in marine environments and HNS spills in marine and atmospheric environments.

- 3) Risk Assessment for oil and HNS spills. The hazard and vulnerability previously obtained are integrated to assess the risk from spills. As a result, the system provides: i) physical environmental and socioeconomic risk maps for the marine pollution caused by oil spills and ii) human, environmental and socioeconomic risk maps for the marine and atmospheric pollution caused by HNS spills.

The outputs will be available within the Decision Support System (DSS) platform.

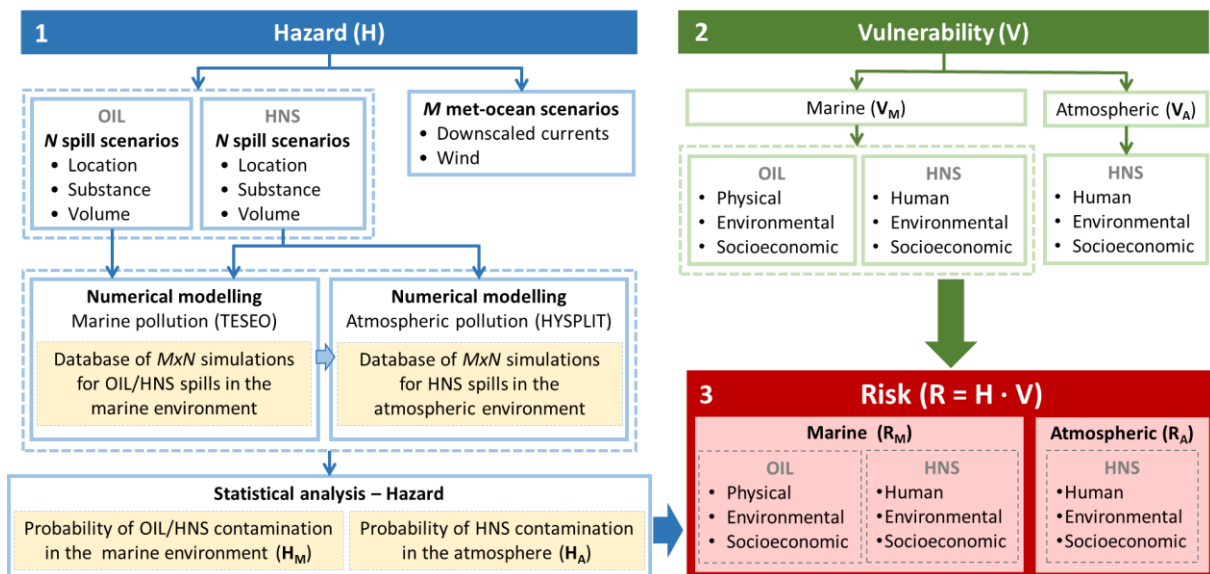


Figure 14 - Risk assessment model.

4.1.1.1. Hazard

The hazard study is carried out by the statistical analysis of a hypothetical oil and HNS spill database generated the simulations described in section 3.1.

Thus, a total of 552 spill simulations have been carried out in the Port of Genoa (combination of 23 metocean conditions, 11 oil scenarios and 13 HNS scenarios), 1850 spill simulations in the Port of Tripoli (combination of 25 metocean conditions, 30 oil scenarios

and 44 HNS scenarios) and 1525 spill simulations in the Port of Aqaba (combination of 25 metocean conditions, 29 oil scenarios and 32 HNS scenarios).

The probability of a specific area being affected by a spill scenario (defined by the spill location, substance and volume) is calculated according to the probabilities of its corresponding met-ocean condition (P^{C_i}). For each Lagrangian simulation, an auxiliary grid is used to count the simulation particles at the surface. The probability of contamination P_{cont} , in the i -th grid cell is obtained as follows:

$$P_{cont} = \sum_{i=1}^{N_c} P^{C_i} \cdot P_i (0,1) \quad (34)$$

where N_c is the number of met-ocean scenarios, P^{C_i} is the probability of occurrence of the met-ocean condition (C_i) and P_i is a binary variable indicating the presence or absence of any particle within cell i :

$$P_i = \begin{cases} 0, & \text{if no particle lies inside the } i - \text{th cell} \\ 1, & \text{if any particle lies inside the } i - \text{th cell} \end{cases}$$

4.1.1.2. Vulnerability

Oil spill vulnerability assessment

The aim of this analysis is to obtain a database that quantifies the vulnerability in the pilot sites to be able to evaluate the risk. The vulnerability assessment is carried out considering the physical, biological and socio-economic resources of the sites by means of different indexes, following the methodology proposed by Abascal et al., 2015; 2022.

- **Physical index (P)**. P is based on ESI (Environmental Sensitivity Index) (Petersen et al., 2002), assesses the potential impact of an oil spill based on the ease of clean-up, depending on the relative exposure to wave energy and the slope of the seabed (beaches, rocks, cliffs and vertical dikes) (Table 7).

Table 7 - Physical vulnerability levels.

Wave exposure	Coast slope	Physical vulnerability	
Exposed	Cliff or vertical dike	Very low	1
	Rock	Low	2
	Beach		
Semi-exposed	Cliff or vertical dike	Medium	3
	Rock		
	Beach	High	4
Sheltered	Cliff or vertical dike		
	Rock	Very high	5
	Beach		

- Environmental index (E). E is estimated based on the protected species and habitats existing in an area: Conservation Areas (e.g., national and natural parks), Habitats of Community Interest (e.g., Site of Community Importance (SCI), Special Area of Conservation (SAC), and Special Protection Area (SPA)) and threatened species.

Table 8 - Environmental vulnerability levels.

Protected species/habitats	Environmental vulnerability	
No conservation areas	Low	2
Conservation areas	Medium	3
Non-Priority Special Area of Conservation or Site of Community Importance	High	4
Priority Habitat of Community Interest or Threatened species	Very high	5

- Socio-economic index (SE). SE is defined to assess the potential impact of an oil spill based on the duration of the interruption of the socio-economic activities located in the study area (Abascal et al., 2015) (Table 9).

Table 9 - Socio-economic vulnerability levels.

Activity interruption	Socio-economic vulnerability	
Activity interrupted by a large surface pollution (slick) – Several days of interruption	Very low	1
Activity interrupted by a surface pollution (patches or patties) - Several weeks of interruption	Low	2
Activity interrupted by a surface pollution (tarballs) - Several weeks to months interruption	Medium	3
Activity interrupted by a light surface pollution (diffuse tarballs) - Several months to one-year interruption	High	4
Activity interrupted by invisible trace of oil (dissolve) - One year or more	Very high	5

HNS spill vulnerability assessment

The vulnerability for HNS spills is assessed from a human, environmental and socio-economic point of view:

- Human index (H). H is determined considering the different activities performed in each area (fisheries, aquaculture, port areas), as well as the distribution of human settlements and the population vulnerability (Table 10).

Table 10 - Human vulnerability levels.

Human activities/uses	Human vulnerability	
Without uses/activities	Very low	1
Fisheries, aquaculture areas, port uses	Low	2
Non-populated areas	Medium	3
Populated areas	High	4
Sites with vulnerable population	Very high	5

- Environmental index (E). E is estimated, such as for oil spills, based on the protected species and habitats existing in an area: Conservation Areas (e.g., national and natural parks), Habitats of Community Interest (e.g., Site of Community Importance (SCI), Special Area of Conservation (SAC), and Special Protection Area (SPA)) and threatened species.

- **Socio-economic index (SE).** SE is based on the potential impact of water pollution (both surface water and water column) on the main socio-economic activities (Legrand et al., 2017) (Table 11).

Table 11 - Socio-economic vulnerability levels.

Socio-economic activity	Socio-economic Vulnerability	
Ports	Low	2
Marinas	Medium	3
Aquaculture	High	4
Tourism Recreational beaches	Very high	5

4.1.1.3. Risk

Once the hazard and vulnerability at the study sites are known, risk assessment can be carried out using the equation:

$$R = H \cdot V$$

As a preliminary step to obtaining risk (R), the hazard values are standardized on 5 levels (Table 12).

Table 12 - Hazard levels.

Hazard ranges	Hazard level	
0	No hazard	0
0 - 10%	Very low	1
10% - 30%	Low	2
30% - 60%	Medium	3
60% - 100%	High	4

Consecutively, a risk weight (RW) is assigned to each possible result of the product of the hazard level (H) and the different vulnerability indexes (V), as is shown Table 13.

Table 13 - Risk weights.

H · V	0	1	2	3	4	5	6	8	9	10	12	15	16	20
Risk weight	0	1	2	3	4	5	6	7	8	9	10	11	12	13

Next, the following criteria is applied in order to obtain the standardized risk (R) for each risk weight, which results in the values presented in Table 14.

$$R = \begin{cases} 0 & \text{if } RW = 0 \\ \text{round} \left(\frac{RW - \min(RW)}{\max(RW) - \min(RW)} \cdot (n\text{classes} - 1) + 1 \right) & \text{if } RW \neq 0 \end{cases}$$

Where

- *round* is a function that rounds the result to the nearest integer
- $\min(RW)$ is the minimum non-zero risk weight (1 in this case)
- $\max(RW)$ is the maximum risk weight (13 in this case)
- *nclasses* is the number of desired standardized risk levels (5 in this case)

Table 14 - Standardized risks.

H · V	0	1	2	3	4	5	6	8	9	10	12	15	16	20
Risk weight	0	1	2	3	4	5	6	7	8	9	10	11	12	13
Standardized risk	0	1	1	2	2	2	3	3	3	4	4	4	5	5

As a result, 5 standardized risk levels (R) can be determined by multiplying the hazard level and the vulnerability (see Table 15).

Table 15 - Risk levels.

H · V	Risk	
0	No risk	0
1 - 2	Very low	1
3 - 5	Low	2
6 - 9	Medium	3
10 - 15	High	4
16 - 20	Very high	5

4.1.1.4. Results

The Risk Assessment model provides the following results for oil and HNS spills in the marine and atmospheric environment:

For oil spills:

- i. Hazard maps for each spill scenario.
- ii. Estimated time of arrival maps for each spill scenario.
- iii. Vulnerability maps: Physical, Environmental and Socioeconomic vulnerability maps.
- iv. Risk maps: Physical, Environmental and Socioeconomic risk maps.

For HNS spills:

- i. Hazard maps for each spill scenario.
- ii. Estimated time of arrival maps for each spill scenario.
- iii. Vulnerability maps: Human, Environmental and Socioeconomic vulnerability maps.
- iv. Risk maps: Human, Environmental and Socioeconomic risk maps.

The outputs will be available within the DSS platform.

As mentioned in section 1.2 and Figure 5, the risk from oil and chemical spills in the marine environment is estimated in the port of Genoa as a new implementation in the framework of PROMPT project. In addition, the risk assessment carried out in Aqaba and Tripoli in the framework of the BE-READY project will be updated taking into account the new high-resolution wind databases developed in PROMPT.

As an example, some results obtained after applying the methodology in the port of Genoa, are shown.

- **ETA and Hazard:**

A post-process analysis of the scenarios modelled by TESEO allows to evaluate the Estimation Time of Arrival, defined as the time after which the slick reaches a particular area, and the Hazard, defined as the probability that the slick reaches a certain area. The two descriptors are plotted in Figure 15, both for a HNS and oil spill. The HNS spill never goes out of the port in the 23 scenarios analysed due to the fact that the chemicals simulated either evaporated or get stuck along the ports structures. While for the oil spill, there are two scenarios in which the slick leaves the port and could potentially damage the surrounding marine environment, but with a very low hazard or probability of occurring.

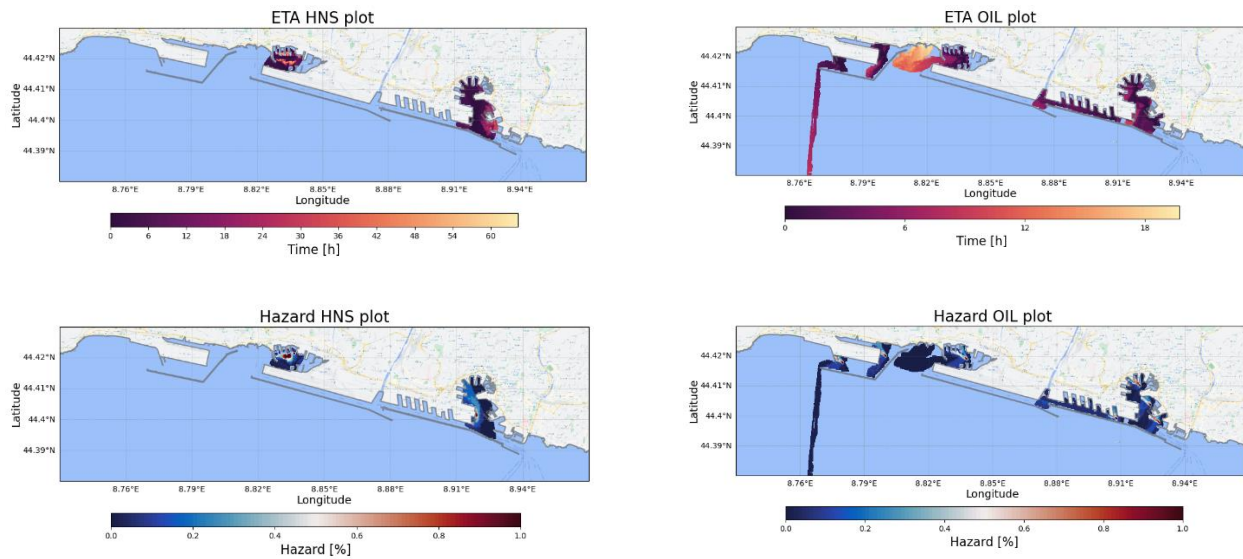


Figure 15 - ETA and hazard map for the HNS (on the left), and for the Oil (on the right).

- Vulnerability:**

As an example, two of the vulnerability indexes obtained in the Port of Genoa are shown, the physical index for oil spills (Figure 16) and the environmental index for oil and HNS spills (Figure 17).



Figure 16 - Physical vulnerability index for water pollution from OIL spills in the Port of Genoa.



Figure 17 - Environmental vulnerability index for water pollution from OIL/HNS spills in the Port of Genoa.

5. DECISION SUPPORT SYSTEM (DSS)

A key objective of this project is to provide decision-makers with a practical tool to assess pollutant dispersion and support timely response actions. To achieve this, a web-based platform has been developed, enabling users to run interactive simulations of pollutant transport in both the marine and atmospheric environments. Through an intuitive interface, users can define spill scenarios by specifying pollutant type, release location, and quantity. The platform integrates real-time environmental data, allowing users to simulate site-specific conditions and track how pollutants spread in both the sea and atmosphere. Outputs include detailed visualizations of dispersion pathways, weathering effects, and affected areas, empowering users to evaluate potential risks and design tailored response strategies. In the following section, a step-by-step guide to run a simulation through the DSS is presented.

1. **Selecting the area of interest.** The first step is to choose the geographical area where the simulation will take place (Figure 18). This can be done by navigating the interactive map and selecting the relevant region.

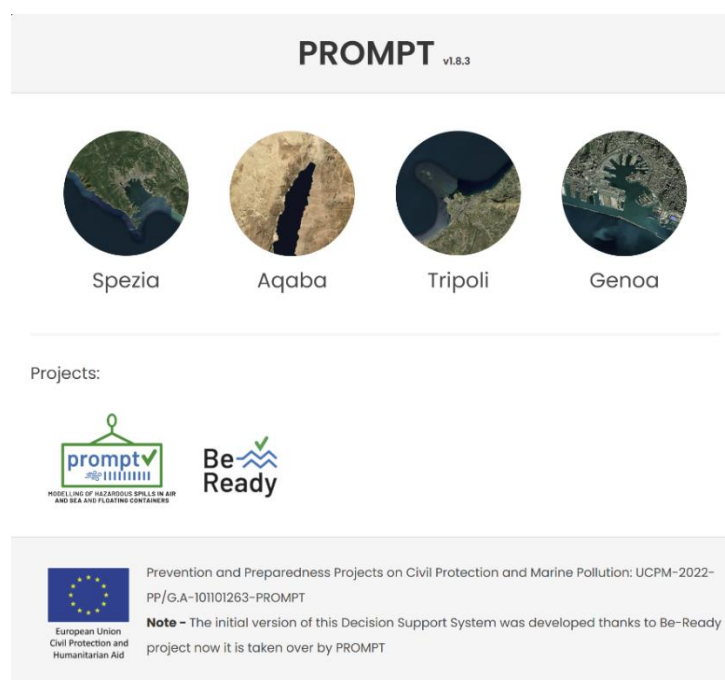


Figure 18 - Selecting the area of interest

2. **Defining the spill characteristics.** Through an intuitive interface (Figure 19), the user specifies key details about the spill

[New simulation](#)
[Show simulation](#)

[Oil](#)
[HNS](#)

Longitude

Latitude

Substances

--- Select a substance ---

Volume (m³)

Simulation day

Simulation hour

Hours of duration

Cluster

--- Select a cluster ---

Water temperature (°C)

Air temperature (°C)

Density (kg/m³)

Result time step

15 minutes

Run simulation

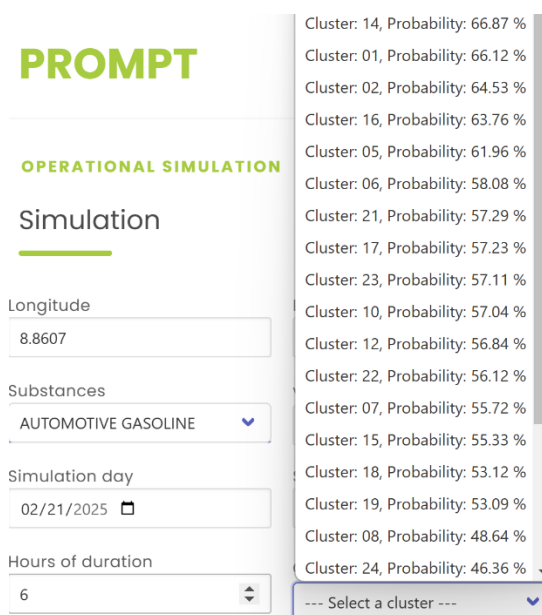
Figure 19 - TESEO simulation form at PROMPT DSS

Table 16 - List of available substances for forecast on-demand in PROMPT DSS

Substance name	
Oil	HNS
FUEL OIL N1-KEROSENO	CRUDE SOY OIL
AUTOMOTIVE GASOLINE	ACETONE
AVIATION GASOLINE 80	ACETIC ACID
BELIDA	ALFAMETHYLSTYRENE
BEKOK	BENZENE
FUEL OIL N1-DIESEL	BUTANE
BRENT BLEND	CYCLOHEXANE
ARABIAN EXTRA LIGHT	CUMENE
FORTIES BLEND	ETHANOL

FUEL OIL N2-DIESEL	ETBE
ARABIAN LIGHT	PHENOL
PRUDHOE BAY	GLYCERIN
TIA JUANA	METHANOL
FUEL OIL N6	METAXYLENE
LAGUNILLAS	MONETHYLENE GLYCOL
	MTBE
	ORTHOXYLENE
	PARAXYLENE
	PROPANE
	PROPYLENE
	CAUSTIC SODA 50%

3. **Choosing the simulation scenario.** The system automatically analyzes real-time meteorological and oceanographic forecasts and ranks pre-computed scenarios based on their similarity to current conditions. The user is presented with a list of scenarios ordered by relevance, with a percentage indicating how closely each one matches the latest daily forecast (Figure 20).



PROMPT

OPERATIONAL SIMULATION

Simulation

Longitude
8.8607

Substances
AUTOMOTIVE GASOLINE

Simulation day
02/21/2025

Hours of duration
6

Cluster: 14, Probability: 66.87 %
Cluster: 01, Probability: 66.12 %
Cluster: 02, Probability: 64.53 %
Cluster: 16, Probability: 63.76 %
Cluster: 05, Probability: 61.96 %
Cluster: 06, Probability: 58.08 %
Cluster: 21, Probability: 57.29 %
Cluster: 17, Probability: 57.23 %
Cluster: 23, Probability: 57.11 %
Cluster: 10, Probability: 57.04 %
Cluster: 12, Probability: 56.84 %
Cluster: 22, Probability: 56.12 %
Cluster: 07, Probability: 55.72 %
Cluster: 15, Probability: 55.33 %
Cluster: 18, Probability: 53.12 %
Cluster: 19, Probability: 53.09 %
Cluster: 08, Probability: 48.64 %
Cluster: 24, Probability: 46.36 %
--- Select a cluster ---

Figure 20 - Choosing the simulation scenario

4. Running the simulation and viewing the results. Once all parameters are set, the user initiates the simulation. The results are displayed on the platform (Figure 21):

- **Map Visualization:** the map dynamically illustrates the evolution of the contaminant over time. Depending on the selected visualization mode, the user can either track individual particles as they move, or observe the concentration field of the pollutant spreading throughout the simulation.
- **Weathering Module Output:** on the left side of the interface, a graph presents the evolution of the pollutant's physical and chemical properties. For example, in the case of a light fuel spill, the system predicts that 80% of the substance evaporates within the first 6 hours of simulation.

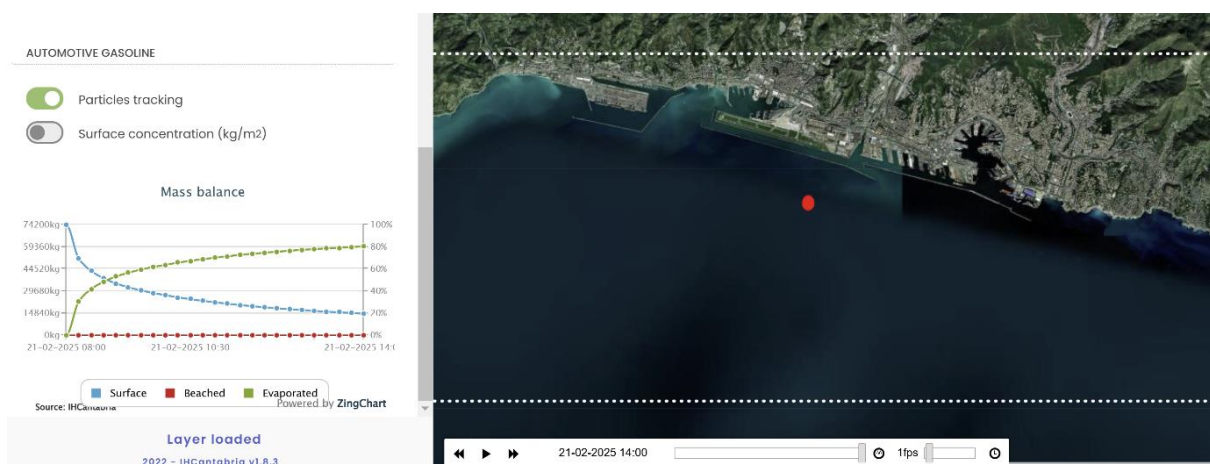


Figure 21 - Results of the simulation

In Aqaba and Tripoli sites, the modelling of atmospheric pollution derived from the evaporation of chemicals is implemented. In these sites, once the marine pollution simulation requested by the user ends, PROMPT DSS will detect if the chemical spill is a candidate to produce a toxic emission into the atmosphere. Eventually, a pop-up window will ask the user to allow the execution of the atmospheric pollution model (HYSPLIT).

PROMPT

Simulation Metocean Risk Hazard Vulnerability

OPERATIONAL SIMULATION - tripoli -

Simulation

New simulation Show simulation

UUID	Date	Cluster
962941b5	11/8/2022, 10:37:49	16
41a0edc6	11/8/2022, 10:38:09	16
aad91d37	3/11/2022, 15:16:10	17
9a93f968	31/5/2023, 11:34:47	17
859037ce	1/6/2023, 13:57:25	04

FUEL OIL NI-DIESEL

- ☒ Particles tracking
☐ Surface concentration (kg/m²)

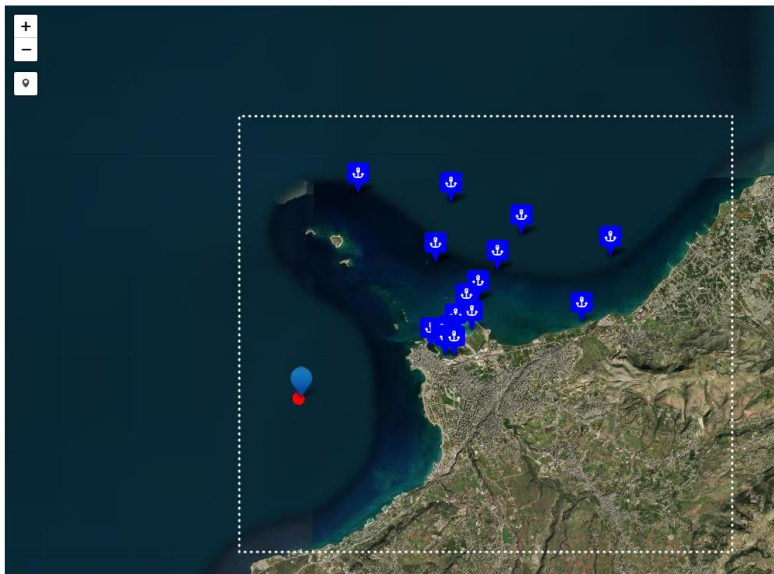


Figure 22 - Example of TESEO's trajectory results in Tripoli port area

PROMPT Simulation Metocean Satellite Risk Hazard Vulnerability

OPERATIONAL SIMULATION - spezia -

Simulation

New simulation Show simulation

UUID	Date	Cluster
253f32dc	2/7/2024, 8:31:12	17
d5fa3b09	13/8/2024, 14:17:41	03
c77a01ba	25/8/2024, 10:26:40	03
da3a0d71	25/8/2024, 11:10:07	06
e0721d61	25/8/2024, 11:16:56	15

AUTOMOTIVE GASOLINE

☒ Particles tracking
☐ Surface concentration (kg/m²)

Mass balance

Layer loaded

2022 - IH cantabria v1.8.0

This simulation evaporates substance into the atmosphere.
Press "Yes" to run the atmospheric simulation.

Yes No

62-07-2024 09:30

100%

1400kg 1500kg 1000kg

0% 50% 100%

Figure 23 - Pop-up window to launch atmospheric pollution simulation of the evaporated part of the substance

Automatically, if the user decides to launch the simulation, a request will be sent to the IHCantabria server that host the HYSPLIT API to run this simulation. The user does not need to define any parameter of the simulation, which will be carried out with the metocean scenario (cluster) defined in the marine pollution simulation; emission configuration is set directly based on the results of marine dispersion.

The results of the Atmospheric pollutant simulation will be the concentration maps of the pollutant between 0 m and 10 m and between 0 m and 50 m, over the mean sea level.

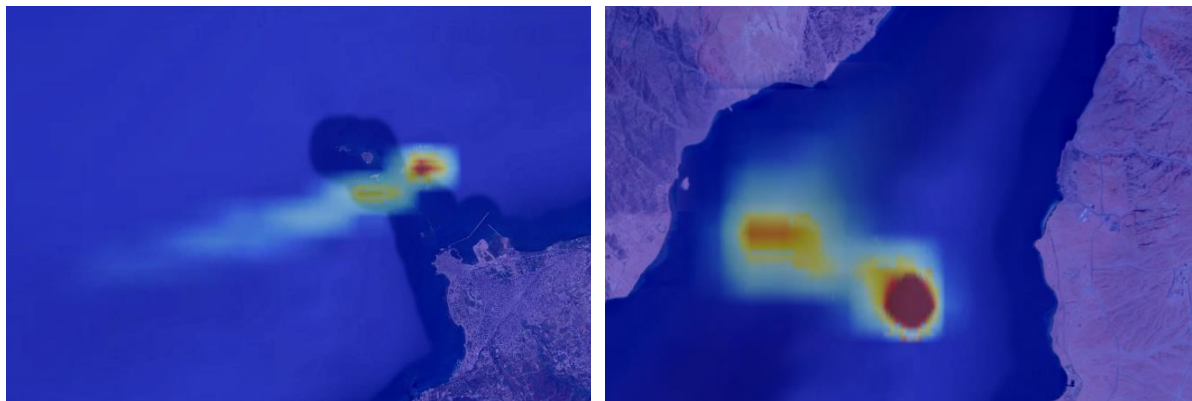


Figure 24 - Example of pollutant concentration between 0 and 10 m over the sea surface at Tripoli (left) and Aqaba (right) port area

This Decision Support System (DSS) is designed to be user-friendly and accessible to both experts and non-experts. By providing a fast and reliable way to predict contaminant dispersion, it enables authorities and response teams to take timely and informed actions in case of environmental incidents.

Beyond simulating the evolution of spill concentration, as detailed in Chapter 4, the DSS provides a comprehensive set of outputs for both hydrodynamic and atmospheric contamination:

- **Estimation Time of Arrival (ETA) Maps:** these maps predict when and where the contaminant will reach specific locations, helping authorities anticipate and mitigate potential impacts.
- **Vulnerability Maps:** by overlaying environmental and socio-economic data, the system identifies the most sensitive areas at risk, such as marine ecosystems, coastal infrastructure, or populated regions.



- **Risk Maps:** combining contamination forecasts with vulnerability analysis, these maps provide a risk assessment framework, allowing decision-makers to prioritize response actions based on the severity and likelihood of impact.



6. METHODOLOGY SUMMARY

Metoccean Modelling

Chapter 2 described the hydrodynamic and atmospheric models, which are fundamental for understanding the movement of pollutants in the marine environment. These models not only provide the essential framework for simulating pollutant transport but also ensure high-resolution accuracy by incorporating local environmental variables.

The hydrodynamic model delivers high-resolution simulations of ocean currents, seamlessly integrating bathymetry, coastal morphology, and key external forcings such as tides and winds. By capturing small-scale processes and fine spatial details, this model ensures precise predictions of current patterns, eddies, and transport pathways. Such detailed outputs are indispensable for pollutant dispersion models, determining how and where substances spread in the water.

On the other hand, the atmospheric model simulates wind fields, temperature, and weather conditions, offering a critical layer of information for pollutants affected by air-sea interactions. This is particularly relevant for volatile and semi-volatile substances, such as hazardous and noxious substances (HNS) or light oil, which can transition between the water and the atmosphere. By integrating wind dynamics with the hydrodynamic model, the system provides a comprehensive picture of dispersion across both marine and atmospheric domains, extending its applicability to complex spills involving multiple transport mechanisms.

Pollution Modelling

Chapter 3 delved into the modeling of pollutant dispersion, specifically focusing on oil and hazardous and noxious substances (HNS), providing essential tools to assess and mitigate the risks of pollution incidents in marine and coastal environments.

For marine pollution, the advection-diffusion module lies at the core of the pollutant modeling system. This module predicts the transport and spreading of substances in the water, accounting for key processes such as advection by ocean currents and turbulent diffusion. To complement this, the weathering module simulates the time-dependent transformation of pollutants. Processes such as evaporation, dissolution, emulsification, and beaching are dynamically modeled, ensuring that the behavior of pollutants is accurately captured from the moment of release to their eventual fate.

Similarly, atmospheric pollution modeling, only applied in Aqaba and Tripoli domains, extends the analysis to airborne dispersion, capturing the behavior of volatile

substances released into the air. This module predicts how pollutants disperse over time and space, considering atmospheric dynamics such as wind speed, direction, and turbulence. The ability to simulate these processes is crucial for highly volatile substances, enabling users to assess risks to both marine and coastal areas. For instance, the model quantifies potential impacts on air quality, and human health, ensuring a comprehensive understanding of pollutant dispersion beyond the marine environment.

A schematic resume of the different numerical models used is reported in the following table:

Table 17 - Models results and application

Numerical modelling	Results	Applied in	Temporal [h]/ Spatial [m] Resolution	Temporal Window	PROMPT innovation	Used in
Hydrodynamic	Currents fields	- Aqaba - Genoa - La Spezia - Tripoli	- 1/25-400 - 1/50-250 - 1/30-80 - 1/25-165	One week	- No - Yes - No - No	Feed marine pollution model (on-demand and risk assessment); DSS metocean module (end user);
Atmospheric	Winds fields	- Aqaba - Tripoli	- 1/1100 - 1/1100	5 days	- Yes - Yes	Feed marine pollution model (on-demand and risk assessment); Feed atmospheric pollution model DSS metocean viewer (end user)
Marine pollution	Oil and HNS spill tracking; Oil and HNS spill weathering evolution; Oil and HNS spill surface concentration;	- Aqaba - Genoa - La Spezia - Tripoli	- 1/270 - 1/40 - 1/50 - 1/55	One week	- No - Yes - No - No	Feed atmosphere pollutant simulation (on-demand and risk assessment); DSS on-demand simulation module (end user); DSS risk assessment module (end user);
Atmospheric pollution	Pollutant concentration in atmosphere	- Aqaba - Tripoli	- 1/1100 - 1/1100	5 days	- Yes - Yes	DSS on-demand simulation module (end user); DSS risk assessment module (end user);

Risk Assessment

To enhance decision-making, a risk assessment methodology was incorporated (Chapter 4), providing a structured approach to evaluate the potential impacts of spills. This methodology considers:

- Hazard: The extent and intensity of pollution, identifying areas of highest contamination risk.



- Vulnerability: The sensitivity of impacted ecosystems, resources, and coastal communities.
- Overall Risk: A combined measure of hazard and vulnerability to prioritize response efforts and mitigate damage.

The Decision Support System

By combining high-resolution modeling, risk assessment methodologies, and user-friendly tools, the pollutant modeling framework ensures a holistic approach to pollution management. Users are empowered to simulate realistic scenarios, assess risks in real-time, and optimize response strategies to minimize environmental and socio-economic impacts. This integrated system fosters improved preparedness, swift response, and informed decision-making, ultimately enhancing resilience to pollution incidents in marine and coastal environments.

7. REFERENCES

- Abascal, A.J., Castanedo, S., Gutierrez, A.D., Comerma, E., Medina, R., Losada, I.J., 2007. TESEO, an Operational System for Simulating Oil Spills Trajectories and Fate Processes. Proceedings of Seventeenth International Offshore Ocean and Polar Engineering Conference. The International Society of Offshore Ocean and Polar Engineering, Lisbon, ISOPE, 3, 1751-1758.
- Abascal, A.J., Castanedo, S., Medina, R., Liste, M., 2010. Analysis of the reliability of a statistical oil spill response model. *Mar. Pollut. Bull.* 60 (11), 2099 - 2110.
- Abascal, A.J., Castanedo, S., Nuñez, P., Cardenas, M., Perez-Diaz, B., Medina, R., 2015. A high resolution oil spill risk assessment system at Santander Bay (Spain), Interspill 2015, Amsterdam (Netherlands).
- Abascal, A.J., Castanedo, S., Núñez, P., Mellor, A., Clements, A., Pérez, B., Cárdenas, M., Chiri, H., Medina, R., 2017a. A high-resolution operational forecast system for oil spill response in Belfast Lough, *Marine Pollution Bulletin*, 114, 302-314.
- Abascal, A.J., Sanchez, J., Chiri, H., Ferrer, M.I., Cárdenas, M., Gallego, A., Castanedo, S., Medina, R., Alonso-Martirena, A., Berx, B., Turrell, W.R., Hughes, S.L., 2017b. Operational oil spill trajectory modelling using HF radar currents: a northwest European continental shelf case study. *Mar. Pollut. Bull.* 119, 336–350. <https://doi.org/10.1016/j.marpolbul.2017.04.010>.
- Abascal, A.J., Gonzalez, M., Aragón, G., Largo, A.M., Lamothe, B., Pedraz, L., Pérez-Díaz, B., de los Ríos, A., Martínez, A., Bárcena, J.F., García, J., García, A., Puente, A., Fernández, F., Medina, R., 2022. A Web-Gis operational system for the risk management of marine and atmospheric pollution from hazardous and noxious substances (HNS) spills in harbour areas, Interspill 2022, Amsterdam (Netherlands).
- ASCE, 1996. State-of-the-art review of modeling transport and fate of oil spills, ASCE Committee on Modeling Oil Spills. Water Resources Engineering Division. *Journal of Hydraulic Engineering*, 122(11), 594-609.
- Barker, C.H., Galt, J.A., 2000. Analysis of methods used in spill response planning: trajectory analysis planner TAP II. *Spill Sci. Technol. Bull.* 6 (2), 145–152.
- Berry, A., Dabrowski, T., Lyons, K., 2012. The oil spill model OILTRANS and its application to the Celtic Sea. *Marine Pollution Bulletin*, Vol. 64, pp. 2489–2501.
- Buchanan, I., Hurford, N., 1988. Methods for predicting the physical changes of oil spilled at sea. *Oil and Chemical Pollution*, Vol. 4, No. 4, pp. 311-328.

- Brighton, P.W.M., 1985. Evaporation from a plane liquid surface into a turbulent boundary layer. J. Fluid Mechanics 159:323-345.
- Brighton, P.W.M., 1990. Further verification of a theory for mass and heat transfer from evaporating pools. J. Hazardous Materials 23:215-234.
- Comerma, E., 2004. Modelado numérico de la deriva y envejecimiento de los hidrocarburos vertidos al mar. Aplicación operacional en la lucha contra las mareas negras. Tesis doctoral, Universitat Politècnica de Catalunya.
- Chiri, H., Abascal, A.J., Castanedo, S., 2020. Deep oil spill hazard assessment based on spatio-temporal met-ocean patterns, Marine Pollution Bulletin, 154, 10.1016/j.marpolbul.2020.111123. IF(2020): 5.553, D1 (3/110).
- Fay, J., 1971. Physical processes in the spread of oil on a water surface. Proc. of the Joint Conf. on Prevention and Control of Oil Spill. American Petroleum Institute, Washington, DC, pp. 463-467.
- Fernandes (2014). Activity 3. Task3.3.2: Technical & Scientific Manual - MOHID HNS (Chemical) Spill Module. Report. ARCOPLUS. Improving maritime safety and Atlantic Regions' coastal pollution response through technology transfer, training and Innovation.
- Galt, J.A., Payton, D.L., 1999. Development of quantitative methods for spill response planning: a trajectory analysis planner. Spill Sci. Technol. Bull. 5 (1), 17–28.
- Hayduk, W., Laudie, H., 1974. Prediction of Diffusion Coefficients for Non-electrolytes in Dilute Aqueous Solutions, Jour. AIChE, 28, 611.
- Hunter, J.R., Craig, P.D., Phillips, H.E., 1993. On the use of random walk models with spatially variable diffusivity. J. Comp. Phys., Vol. 106, pp. 366-376.
- Kawamura, P. I., Mackay, D., 1987. The evaporation of volatile liquids. J. Hazardous Materials 15:343-364.
- Kolluru, V.S., 1992. Influence of Number of Spilllets on Spill Model Predictions. Applied Science Associates Internal Report
- Legrand S., F. Poncet, L. Aprin, V. Parthenay, E. Donnay, G. Carvalho, S. Chataing-Pariaud, G. Dusserre, V. Gouriou, S. Le Floch, P. Le Guerroue, Y.-H. Hellouvy, F. Heymes, F. Ovidio, S. Orsi, J.Ozer, K. Parmentier, R. Poisvert, E. Poupon, R. Ramel, R. Schallier, P. Slangen, A. Thomas, V. Tsigourakos, M. Van Cappellen and N. Youdjou (2017) "Mapping Environmental and Socio-Economic Vulnerability to HNS Maritime Pollution", HNS-MS final report, part III, 122 pp

- Lehr, W.J., 2001. Review of modeling procedures for oil spill weathering behavior. Oil Spill Modelling and Processes, C. A. Brebbia Ed., WIT Press, pp. 51-90.
- Mackay, D., Matsugu, R.S., 1973. Evaporation rates of liquid hydrocarbon spills on land and water. Can. J. Chem. Eng. 51:434-439.
- Mackay D., Leinonen P.J., 1977. Mathematical model of the behaviour of oil spills on water with natural and chemical dispersion. – Rapport technique n° EPS-3-EC-77-19, Fisheries and Environmental Canada,
- Mackay, D., Paterson, S., Trudel, K., 1980. A Mathematical Model of Oil Spill Behaviour. Environmental Protection Service, Fisheries and Environment Canada, EE-7, 39p.
- Mackay, D., Paterson S., Nadeau, S., 1980. Calculation of the evaporation rate of volatile liquids. Proc. of the National Conference on Control of Hazardous Material Spills, Louisville, KY, pp. 361-367.
- Mackay, D., Shiu, W.Y., Hossain, K., Stiver, W., McCurdy, D., Petterson, S., Tebeau, P. A., 1983. Development and Calibration of an Oil Spill Behavior Model, Report No. CG-D-27-83, United States Coast Guard Office of Research and Development, Groton, Conn., USA.
- NOAA, 1994. ADIOS. Automated Data Inquiry for Oil Spills. User's Manual (see 1.1). NOAA/Hazardous Materials Response and Assessment Division, Seattle, Washington.
- Petersen, J., Michel, J., Zengel, S., White, M., Lord, C., Plank, C., 2002. Environmental Sensitivity Index Guidelines, Version 3.0.
- Rasmussen, D., 1985. Oil spill modelling - a tool for cleanup operations. Proc. 1985 Oil Spill Conf., American Petroleum Institute, Washington, D.C., pp. 243-249.
- Reed, M., Gundlach, E., y Kana, T., 1989. A coastal zone oil spill model: development and sensitivity studies. Oil and Chemical Pollution, Vol. 5, No. 6, pp. 451-476.
- Reynolds, R. M., 1992. ALOHA™ (Areal Locations of Hazardous Atmospheres) 5.0 theoretical description. NOAA Tech. Memo. NOS ORCA-65. National Oceanic and Atmospheric Administration/Hazardous Materials Response and Assessment Division. Seattle, WA.
- Sebastiao, P., and Guedes Soares, C., 1995. Modeling the Fate of Oil Spills at Sea. Spill Science and Technology Bulletin, Vol.2, No. 2/3, pp. 121-131.
- Sotillo, M.G., E. Alvarez Fanjul, S. Castanedo., A.J. Abascal, J. Menendez, R. Olivella, E. García-Ladona, M. Ruiz-Villareal, J. Conde, M. Gómez, P. Conde, A.D. Gutierrez, and R. Medina, "Towards an Operational System for Oil Spill Forecast in the Spanish Waters: Initial Developments and Implementation Test", Marine Pollution Bulletin, 56(4):686-703, 2008.



Stiver, W. & Mackay, D., 1984. Evaporation Rate of Spills of Hydrocarbons and Petroleum Mixtures. Environment Science & Technology, Vol. 18, pp. 834-840.

Thibodeaux, L.G., 1979. Chemodynamics: environmental movement of chemicals in air, water, and soil, New York, John Wiley and Sons.

